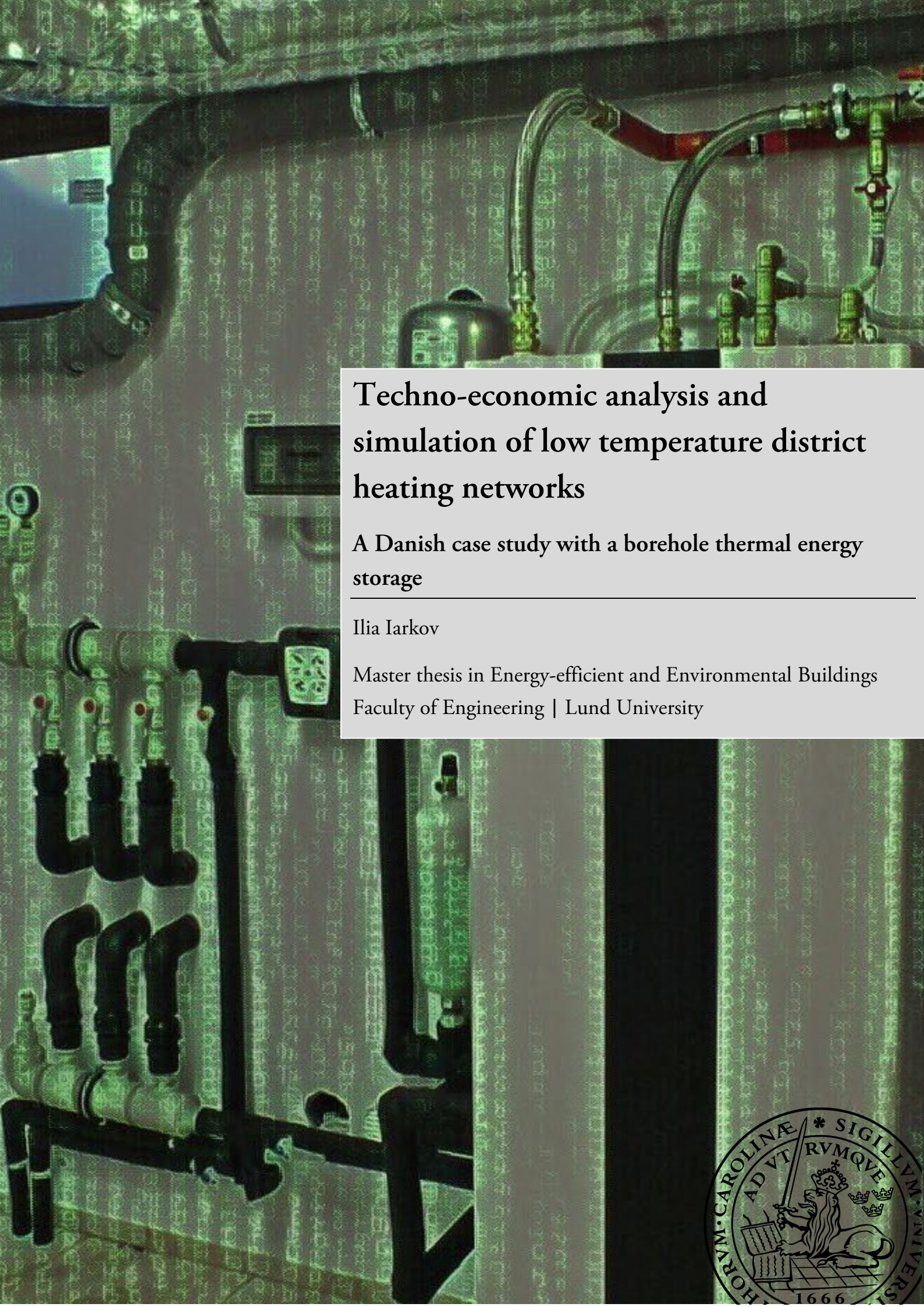

Techno-economic analysis and simulation of low temperature district heating networks

A Danish case study with a borehole thermal energy storage

Ilia Iarkov

Master thesis in Energy-efficient and Environmental Buildings
Faculty of Engineering | Lund University

Lund University

Lund University, with eight faculties and a number of research centres and specialised institutes, is the largest establishment for research and higher education in Scandinavia. The main part of the University is situated in the small city of Lund which has about 112 000 inhabitants. A number of departments for research and education are, however, located in Malmö. Lund University was founded in 1666 and has today a total staff of 6 000 employees and 47 000 students attending 280 degree programmes and 2 300 subject courses offered by 63 departments.

Master Programme in Energy-efficient and Environmental Building Design

This international programme provides knowledge, skills and competencies within the area of energy-efficient and environmental building design in cold climates. The goal is to train highly skilled professionals, who will significantly contribute to and influence the design, building or renovation of energy-efficient buildings, taking into consideration the architecture and environment, the inhabitants' behaviour and needs, their health and comfort as well as the overall economy.

The degree project is the final part of the master programme leading to a Master of Science (120 credits) in Energy-efficient and Environmental Buildings.

Examiner: Saqib Javed (Division of Building Services)

Supervisor: Marwan Abugabbara (Division of Building Services)

Keywords: Low-temperature district heating, Modelica, BTES, LCA, LCC

Publication year: 2023

"There is no way around the hard work. Embrace it. You have to put in the hours because there is always something you can improve. You have to put in a lot of sacrifice and effort for sometimes little reward, but you have to know that, if you put in the right effort, the reward will come."

-Roger Federer

Abstract

The continuous increase in global energy consumption has led to a greater focus on the energy required for heating buildings. This thesis presents a techno-economic model for analysing low-temperature district heating networks coupled with a geothermal heat source. The model was used to analyse an existing system in Denmark with 15 connected single-family detached houses. Each of the houses has a substation with a decentralised heat pump. Measured data was used to validate the model based on the temperature levels at the evaporator side of each building heat pump. The results revealed that the analysed system benefits from using uninsulated pipes, which receive heat gains from the ground, improving the system's temperature quality. However, according to the simulation results, the efficiency of the system and its economic and environmental performance have room for improvement, mainly due to the ground heat depletion problem. From a hydraulics point of view, the simulated system has the potential to function efficiently, having relatively low-pressure drops on the bore field level, which is beneficial for the SPF of the system. Several solutions were proposed to increase the efficiency, and a preliminary direction for future studies was discussed.

Acknowledgements

At the outset of this thesis, I want to state that while my name may stand alone in this work, it is the culmination of a collaborative effort. This journey, filled with trials and triumphs, was made possible through the unwavering support, guidance, and inspiration of countless individuals who have shaped my life and academic journey.

To begin with, my heartfelt appreciation goes out to my supervisor, Marwan Abugabbara. His patience, engaging discussions, provision of the models, indispensable guidance, and relentless encouragement were instrumental in expanding my knowledge and shaping the research presented in this work. I have learned a great deal from him about technical aspects of district heating, modelling and research methods, and his critique has been a crucial asset for my professional growth.

Saqib Javed deserves a special mention for his expertise in district heating and the invaluable resources and feedback he provided, enabling me to fine-tune my ideas and work with more precision. His comments and knowledge were vital for the improvement of this work.

Henrik Davidsson was the torchbearer who lit my path to studying in Sweden, providing guidance and support at every juncture. Without his encouragement and help, I would not be where I am today.

My gratitude extends to Harald Lindström, Anders Söderstrom, Louise Plitz Vitanc, and Matilda Hinsegård, who challenged and encouraged me when it was necessary, and for the lunchtime ping-pong matches.

I am indebted to Lauren Thomson and Stephen Vaughan for standing by me during my most challenging times, demonstrating that there's always another way forward when the path seems narrow.

I cannot adequately express my gratitude to my mother, a beacon of love and encouragement that has consistently guided me through every twist and turn in my journey. Her unwavering support and faith in me have fuelled my determination, even amidst challenges. As an accomplished IT professional, she has been sharing the knowledge with me from my younger years, enriching and enhancing my academic journey. Her invaluable role as a mother, mentor, and guide is integral to my life.

Lastly, I extend my sincere gratitude to the Swedish Institute, whose sponsorship made this entire journey possible. Without their support, my dreams would have remained just that – dreams.

Lund, June 2023

Ilia Iarkov

Table of contents

Nomenclature

Definitions

Brine: an anti-freezing mixture, ethanol in this specific case.

District heating and cooling/District heating and cooling systems: terms used interchangeably throughout the thesis pertaining to the whole system from the heat source to the final user.

District heating and cooling grids/networks: terms used interchangeably throughout the thesis pertaining to the piping system used for delivering space heating and/or cooling to the final user.

District side/Supply side: terms used interchangeably throughout the thesis pertaining to HVAC installations used for the building's heating and/or cooling energy supply.

Demand side/Building side: terms used interchangeably throughout the thesis relating to final heating and/or cooling energy delivery to the building systems.

LTHD: low-temperature district heating. A concept which refers to the district heating systems with low supply temperature (lower than 55 °C), compared to traditional district heating systems, with a supply temperature of 80 °C and above.

Noisy data/unrepresentative data: erroneous data obtained due to various distortions during data collection. Used interchangeably throughout the thesis.

NoSQL database: a data organisation method, referring in this thesis to a data structure with numerous parameters in a single column, accompanied by a separate column of keys that describe each value's type.

Relational database: a data organisation method, referring in this thesis to a data structure with different parameters in separate columns.

Substation: an installation that couples district heating and/or cooling systems with building systems. It can include, e.g., heat pumps, circulation pumps, balancing valves, local distribution pipes, sensors, and controllers.

Abbreviations

COP	Coefficient Of Performance
DHW	Domestic Hot Water
GHSP	Ground Source Heat Pump
GWP	Global Warming Potential
HVAC	Heating, Ventilation, Air Conditioning
HP	Heat Pump
LCA	Life Cycle Analysis
LCC	Life Cycle Costing
NPV	Net Present Value

Latin and Greek letters

c_p	Specific heat capacity	[J/(kg·K)]
d	Diameter	[m]
E	roughness	[m]
E_e	Electrical energy	[kWh] or [MWh]
E_h	Heating energy	[kWh] or [MWh]
h	Head of the pump	[Pa]
$\dot{m}$	Mass flow rate	[kg/s]
P	Electric power	[W] or [kW]
Δp	Pressure drop	[Pa]

$\dot{Q}$	Heating power	[W] or [kW]
T	Temperature	[°C] or [K]
v	Velocity	[m/s]
η	Efficiency	[-]
ρ	Density	[kg/m^3]

Subscripts

br	Brine
cond	Condenser
comp	Compressor
evap	Evaporator
el	Electricity
nom	Nominal
h	Heating
w	Water

1 Introduction

1.1 Background

The building sector is responsible for approximately 30 % of the energy use world-wide (International Energy Agency, 2023). Global energy consumption has increased significantly during the last 70 years, with much of this energy generated by non-renewable sources (Smil et al., 2022). A considerable portion of this energy is being used for heating and cooling buildings (Fleiter et al., 2017), with the forecast of a 50% increase in energy use for cooling by 2030 (International Energy Agency, 2018) and a 20% increase in energy use for heating by 2030 (International Energy Agency, 2022) compared to 2020 if the energy-efficient measures are not in place.

The first measure considered by the research community and industry to reduce energy use was the construction of low-energy buildings, resulting in the emergence of the concepts such as passive houses, zero-emission buildings and plus-energy buildings (Abel, 1994; Karlsson & Moshfegh, 2007; Thomsen et al., 2005). However, most of these works deal mainly with the new constructions. There have been attempts to increase the energy efficiency of the existing buildings, but they require significant investments, which the decrease in operational energy should repay (Zhu et al., 2009). At the same time, one of the ways to decrease primary energy use and reduce carbon emissions is the transition to renewable energy sources. This issue has been tackled as well, with several successful projects finding different ways to incorporate renewables into the energy system (Fragaki et al., 2008; Lund et al., 2005; Perry et al., 2008; Torchio et al., 2009; Volkova et al., 2020). One promising approach to address this challenge is to focus on developing and improving district heating systems, which can effectively reduce energy waste by decreasing distribution heat losses while meeting the growing demand for heating and cooling (Lund et al., 2010; Werner, 2017).

1.2 Evolution of district heating

District heating systems have been developed over several generations to improve efficiency, reduce emissions, and enhance sustainability. The first-generation systems relied on local coal-fired power plants and used steam as the primary heat carrier. These systems were highly polluting and inefficient due to the environmental damage of the coal combustion and the high temperatures of the transportation fluid. Second-generation systems, developed at the beginning of the 20th century, featured larger and more efficient centralised plants and pressurised water as a primary heat carrier with a supply-side temperature above 100 °C, leading to significant heat losses from the pipes (Thorsen, Gudmundsson, et al., 2020). Third-generation heating systems, which were introduced in 1980, featured the possibility of having smaller centralised plants but also featured small substations. The substations are the installations which couple district heating and/or cooling systems with building systems and can include, e.g., heat pumps, circulation pumps, balancing valves, local distribution pipes, sensors, and controllers. The possibility of individual metering of the energy use and integration of renewable energy also characterised this type of system. However, these systems still had a high temperature on the supply side, reaching 80 °C, contributing to high heat losses (Thorsen, Gudmudsson et al., 2020).

A recent development in district heating sustainability evolved in two separate directions - Smart Energy systems development, which began in 2011 (Lund et al., 2011) and fourth-generation district heating systems, conceptualised in 2014 (Lund et al., 2014). The Smart Energy System approach was based on the Smart electricity grids (Lund et al., 2012). However, unlike the latter, it incorporated a holistic and cross-sectoral approach. It advocated for the gradual transition to renewable energy sources from fossil fuels in every industry. Three scenarios for gradual decarbonisation were proposed – a conservative approach, which considered only the existing technologies, an ideal approach, which considered a significant advance in the technology sector and a recommended approach, which combined the elements of both approaches (Lund et al., 2011). Some of the proposed measures were implemented in Denmark, gradually decreasing primary energy use in the past ten years (Fulghum, 2023). The Smart Energy System approach offers, however, certain disadvantages, such as a limited potential to use flexible electricity demand, high costs, especially for industrial users, and unbalanced day-night electricity usage (Kwon & Østergaard, 2014; Ropenus & Klinge Jacobsen, 2015). This led to the conclusion that the complete green transition should encompass electricity, heating, and cooling systems (Connolly et al., 2016; Nastasi & Lo Basso, 2016).

Fourth-generation district heating systems (4GDH) are still being developed. These systems introduced low-temperature grids, which can use heat sources at temperatures as low as 55 °C – 65 °C, significantly expanding the range of available heat sources. Fourth-generation systems also increased the use of renewable energy sources, such as biomass and geothermal energy, and focused on improving the system's overall efficiency (Lund et al., 2014). A significant advantage of 4GDH is integrating renewable energy sources and waste heat from industrial applications (Fang et al., 2015; Lottner et al., 2000; Ozgener et al., 2005). This leads to the main benefits of fourth-generation district heating systems: increased energy efficiency, reduced CO_2 emissions, improved energy security, and lower end-user costs. (Averfalk & Werner, 2020; Sayegh et al., 2017).

Another concept which emerged within the 4GDH is low-temperature district heating (LTDH). LTDH systems operate at lower temperatures than traditional district heating systems, going as low as 40°C on the supply side. The temperature which comes to the building in these systems is regulated by the domestic hot water instead of heating (Schmidt et al., 2017). However, the economic feasibility of such systems, at the current level of development, is uncertain due to the additional equipment required for such systems, as shown by case studies in Canada (Dalla Rosa et al., 2012), Denmark (Ommen et al., 2016), and Japan (Baldvinsson & Nakata, 2016). Another risk associated with low-temperature district heating systems is the potential for the growth of Legionella bacteria. Legionella is a waterborne bacterium that can cause Legionnaires' disease, a severe form of pneumonia. Legionella bacteria thrive at 30 °C – 46 °C with a breakpoint of 55 °C – 60 °C (Mathys et al., 2008). This concern was addressed in the scientific literature on the example of a Danish house. Two main solutions to this issue were proposed, involving centralised and decentralised substations. It was concluded that the decentralised substations coupled with heat pumps could eliminate the risk of Legionella and reduce distribution losses by 30% (Yang et al., 2016). However, these substations invoke additional investment costs.

Fifth-generation district heating systems (5GDH) represent the next step in the evolution of district heating technology. These systems are designed to be even more efficient and sustainable than previous generations, using a combination of advanced technologies, such as renewable energy sources, waste heat recovery, energy storage, and smart control systems. A common characteristic among these systems is the use of thermal networks capable of supplying and extracting heat at low temperatures, typically to operate heat pumps for heating and/or cooling purposes at the end-users. This definition of 5GDH is used in this thesis. The key feature of the 5GDH is sharing heating and cooling energy between the buildings connected to the system (Lindhe et al., 2022; Lund et al., 2021; Wirtz et al., 2022). The main benefits of fifth-generation district heating systems are their increased use of renewable energy sources and waste heat recovery and their ability to integrate with other energy systems, such as electricity grids. Additionally, these systems have the potential to provide flexible and responsive heating and cooling solutions, reducing peak demand and avoiding the need for expensive upgrades to the electricity grid. (Buffa et al., 2019)

Despite the potential benefits of fifth-generation district heating systems, their implementation has been limited, and it is challenging to conclude their efficiency. There are too few case studies of their application and a lack of standardised methods for evaluating their performance. One of the main challenges facing the widespread adoption of fifth-generation district heating systems is their economic viability. While these systems have the potential to be more sustainable and efficient, their higher initial costs may make them less attractive to investors and end-users. In some case studies, fourth-generation district heating systems were found to be more cost-effective than fifth-generation systems, making their implementation more attractive. (Gjoka et al., 2023; Gudmundsson et al., 2022; Volkova et al., 2022). However, this research did not consider 5DGH potential for cooling.

One example of the fifth-generation district heating system, Ectogrid, treats the buildings as the producers of heating or cooling energy and conducts an energy exchange between the buildings. Ectogrid, created by E.ON, has established a pilot plant in Lund, Sweden. This innovative system comprises a low-temperature distribution grid that supplies both heating and cooling within a single network, maintaining temperatures between 16 °C and 40 °C in hot pipes and 6 °C and 30 °C in cold pipes. Local chillers and heat pumps ensure appropriate temperature levels for end users, while an air-source heat pump serves as a balancing unit, generating heating or cooling on demand (Lindhe et al., 2022). Another example of a low-temperature district heating system is the system situated in Midtjylland, Denmark. This system employs a group of heat pumps that extract heating energy from a borehole field. The system aims to satisfy the heating and domestic hot water (DHW) requirements through local heat generation while maximising system efficiency. A noteworthy advantage of

this system is the possibility of deployment in areas with low-population density. (Andersen, 2017; Filonenko et al., 2019).

Previous studies have mainly concentrated on the sizing of components and the design of the 5GDH networks, conducting the system analysis regarding thermohydraulic modelling. A design methodology and the optimisation algorithm of the temperature control of 5GDH were proposed, which led to noticeable operational cost savings of the network (Wirtz et al., 2020, 2021). In another study, the potential strategies to connect individual substations to the 5GDH network were evaluated to determine which buildings could be connected to the grid and how it would affect the grid (von Rhein et al., 2019). Other research compared two different network types showing the importance of correctly selecting the topology of the 5GDH (Sommer et al., 2020). Incorporating the new energy structures and their effects was also evaluated, demonstrating how the different energy geostructures interact and affect each other. Nevertheless, according to the author's knowledge, very limited work has been done to analyse 5GDH from a holistic perspective including a multi-domain dynamic model, similarly to the model presented by (Abugabbara et al., 2022). This model was developed for the system with both heating and cooling demands, and no research was conducted on the techno-economic and environmental performance of low-temperature geothermal district heating systems that are solely dedicated to providing heat. Therefore, further investigation into this specific area of study is warranted to assess the performance and potential of the LTDH and assist in decision-making in the field of district heating. Consequently, a Danish LTDH system has been selected for a comprehensive evaluation in this work, addressing this knowledge gap and contributing to a better understanding of its overall effectiveness and potential.

1.3 Aims

This thesis explores an existing case of a low-temperature district heating grid by conducting an in-depth analysis of the low-temperature district heating grid with a bore field thermal energy storage located in Midtjylland, Denmark. The study aims to investigate the system's energy usage, identify potential advantages and disadvantages, and uncover opportunities for enhancement using the equation based object-oriented Modelica language. The necessity of the modelling is outlined in the investigation of the techno-economic and environmental performance from the global perspective with the application of the holistic approach, combining several technical aspects.

The primary objective of this research is to expand the holistic understanding of low-temperature district heating implementation, assess its potential and actual performance and identify the areas of improvement. The examined district heating network type could potentially supplant conventional district heating systems, bolstering national energy security. Moreover, it could be employed in regions where standard district heating grids may not be feasible. The resulting model could assist in the planning stage for analysing and comparing different district heating concepts. The measured data from the existing district heating grid provides inputs for the model and validates its performance.

In pursuit of these objectives, this thesis seeks to address the following research questions:

- What is the expected performance of a low-temperature district heating system coupled with a borehole heat source?
- What are the potential strengths and areas for improvement within the system?
- What are the economic benefits and environmental impacts of the system?

1.4 Scope

This thesis encompasses several areas, including data pre-processing, model assembly, model validation, techno-economic assessment of the model, hydraulic analysis of the system, and life-cycle analysis of the system's energy use. The investigation utilises measured data from a pre-existing system in central Denmark, covering four years from November 2018 to November 2022. It is important to note, however, that the focus of this thesis does not extend to evaluating the accuracy of the pre-developed components of the model, the selection of system components, or system hydraulic balancing.

2 Method

This section describes the evaluated LTDH system, presents a detailed description of the modelling process, and explains the data pre-processing. Furthermore, the section explains the key performance indicators (KPI) selected for the system analysis, describes the model's validation process, and establishes this study's limitations.

2.1 Description of case study

The analysed low-temperature district heating grid is in the Midtjylland area of Denmark. The grid comprises 14 new detached single-family houses and one existing single-family house. The district heating system is coupled with an energy source consisting of six 120 meters deep boreholes forming a bore field. This bore field is the primary and only energy source for each household's heating and domestic hot water needs. The brine was used on the supply side. The system started in 2018 when 11 new and one old building were connected to the analysed district heating system. One more new building was connected in 2020, and two more were added in 2022 (*Dataindsamling fra danske termonet (HO5)*, 2022).

The schematic of the analysed system is provided in Figure 1. Light blue and yellow figures represent the buildings connected to the system. The colour choice for the building marking was chosen only based on the readability of the schematic. The supply and return pipes are demonstrated on the schematic with red and blue lines, respectively. Every borehole connected to the analysed system is shown with a green circle and a letter from A to F.

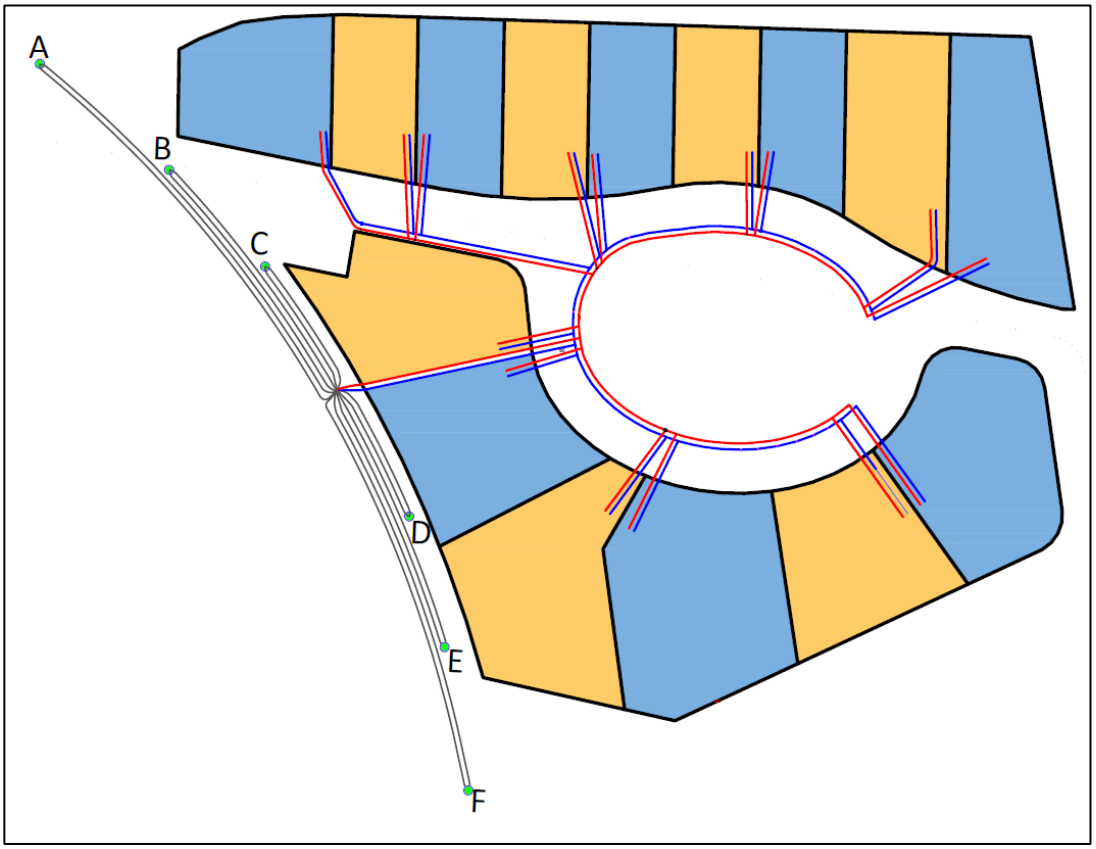

Figure 1: Site plan of the analysed district heating system.

Every new building has a substation with an installed heat pump of a maximum heating effect of 5.8 kW. The old building was equipped with a similar substation, with a maximum heating effect of 10.2 kW. The substation heat pumps work either in space heating mode when they produce water at the temperature of 40 °C and below or domestic hot water mode when they produce water at the temperature above 40 °C. The heat pumps increase the water temperature to 60 °C weekly for legionella protection, independent of the outdoor temperature, heating loads or domestic hot water (DHW) demand. Priority is given to the production of domestic hot water over heating. The heat pumps are also equipped with an auxiliary electric heater, which can be activated if the heat pump's power is insufficient to cover DHW or heating demand.

The heat pump schematic is provided in Figure 2. Each heat pump was equipped with four temperature sensors, which were used to measure brine supply and return temperatures, represented by sensor 1 and sensor 2, respectively, and water supply and return temperatures, denoted by sensor 3 and sensor 4. The data recording from the heat pump was triggered by a change in any of these parameters. For instance, without outdoor temperature fluctuations, the sensors would not register new measurements. Consequently, all values obtained from these sensors were expressed as integer values.

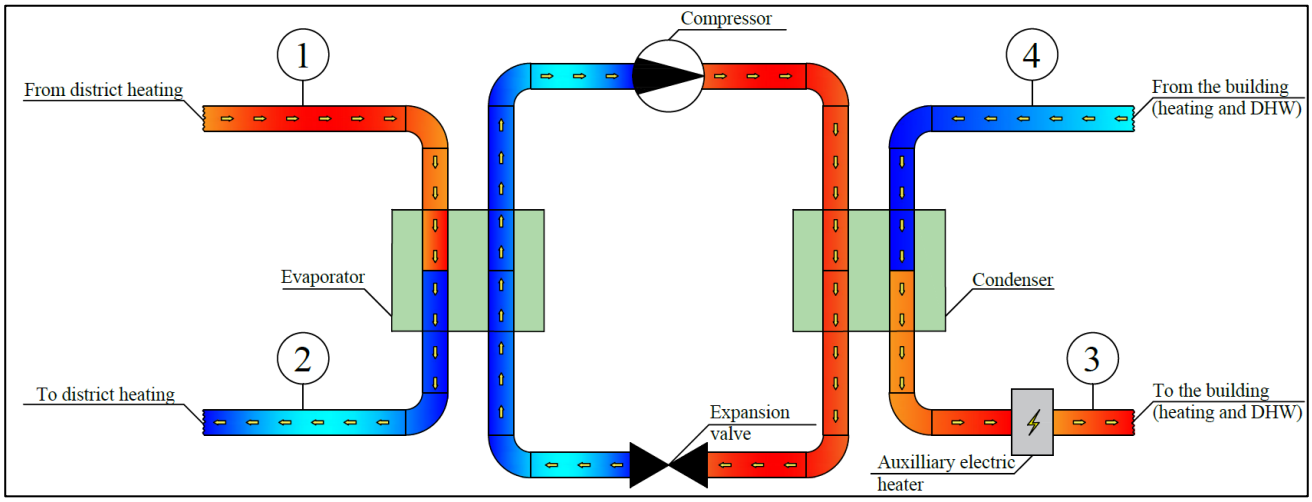

Figure 2: Heat pump schematic.

2.2 Modelling and simulations

The model was developed with Dymola, a simulation environment that enables users to write, compile, and simulate models produced using the Modelica modelling language (Modelica Association, 2023). Dymola offers a wide range of modelling and simulation capabilities, making it an ideal tool for accurate evaluation of the performance of complex systems (Schweiger et al., 2017). Modelica language has been selected due to its precision and flexibility, compared to other equation-based tools (Musić & Zupančič, 2006). More so, the modular structure of this tool allows the users to exchange the models, streamlining the design process. This work primarily uses two publicly available component libraries – Modelica Standard Library and Modelica Buildings Library (Wetter et al., 2014). Modelica has been verified for the dynamic simulations of district heating systems (Lauster et al., 2014) and used for several case studies, including the district heating system in Germany, where a new tool for the hydraulics simulations was developed (Sangi et al., 2017) and a renewable energy district heating system in the Netherlands (Soons et al., 2014). The development of this tool continues to implement more functions for system-level energy simulations (Long et al., 2021). For these reasons, the Modelica programming language was selected for the simulations. In this case, Modelica was employed to examine the performance of the district heating system and the associated substations, allowing for a comprehensive analysis of energy use, heat losses, hydraulics performance and efficiency of the modelled system.

The overall model of the district heating system implemented in Dymola is illustrated in Figure 3, and a brief description of the system components is presented in Table 1. Each component or group of components was designated by a letter. A more detailed explanation for specific components was provided in each component section. The model uses the demand side water temperatures and auxiliary heater power as inputs and calculates the energy load on each substation based on them and the constant water flow due to the presence of a constant speed circulation pump and according to the previous research of similar systems (Liu et al., 2020; *Dataindsamling fra danske termonet (HO5)*, 2022). Based on these loads, the brine flow from the bore field, the brine properties and the brine supply temperature were calculated. The distribution pipe models calculated the heat added or removed from the brine based on the undisturbed ground temperature surrounding the pipes and temperatures of the brine in supply and return district network pipes. The brine properties and flow were transmitted to the substation, and the substation transmitted the brine return temperature and properties back to the distribution pipe model. Then the post-processing of the results was conducted based on the energy use of the system, pipe heat losses or gains and the electric energy use for the auxiliary heater and the compressor of

every substation to determine the seasonal performance factor (SPF), life-cycle costs and the global warming emissions of the purchased energy for the analysed Danish LDTH system.

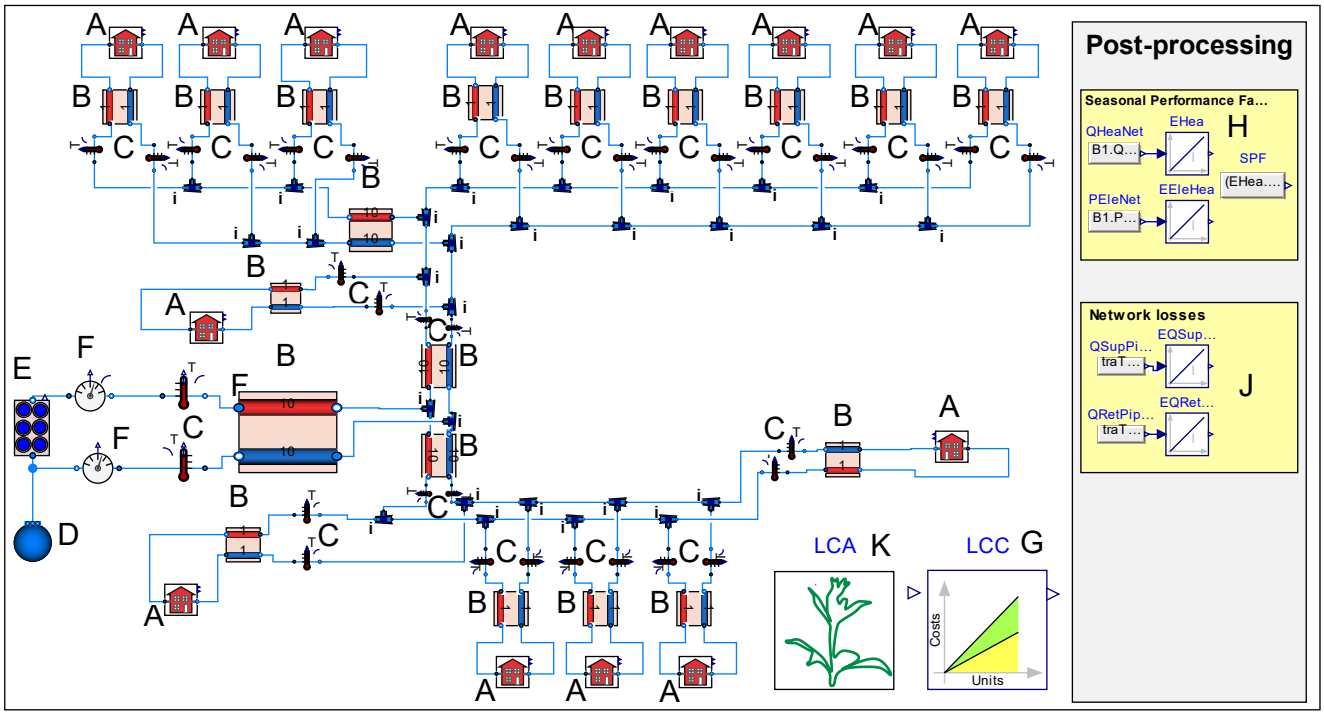

Figure 3: System model schematic.

Table 1: A description of the model components.

Letter	Component	Description
A	Substation	Represents the substation installed in each building connected to the space heating and DHW system. Its detailed schematic and description are provided in section 2.2.1.
B	Double uninsulated pipes	Represents the supply and return pipes from district heating with the symmetric and asymmetric components of heat transfer. Every model represented the segment of the pipe with a different diameter. Its detailed schematic and description are provided in section 2.2.2.
C	Temperature sensors	Calculates the simulated temperature measurements of brine in different system parts.
D	Water source	Creates a fluid (brine) flow in the system and prescribed the temperature and pressure of the source.
E	Borehole model	Calculates the BTES heat exchange and flow. The parameters of this component are explained in Section 2.2.3.
F	Enthalpy sensor	Calculates the heat added/removed to/from the fluid.
G	LCC calculation	Calculates the life cycle costing. Its detailed description is provided in Section 2.2.4.
H	SFP	Calculates the SFP.
I	Mixing junction	Splits the brine flow.
J	Pipe heat losses/gains	Calculates the total heat gains through the uninsulated pipes.
K	LCA	Calculates the environmental impacts of the building. Its detailed description is provided in Section 2.2.5.

2.2.1 Substation model

Each building is equipped with a substation, as illustrated in Figure 4. Component 1 represents the collection of building data as explained in Section 2.3. This component has several variables that are directly used in the calculation (referred to as inputs) and some parameters that are employed to compare the model performance with the existing system (referred to as reference values). The inputs include water supply temperature, water return temperature, heating power, DHW power, and auxiliary heating power. The reference values encompasse outdoor, brine supply, and brine return temperatures. The supply and return temperature information is transferred from the input data to Component 2, where the temperature is converted from Celsius to Kelvin. Subsequently, the return temperature measurement is utilised as an input in Component 3 to calculate the characteristics of water under the prescribed temperature, which is returned to the heat pump from the building side. Component 3 has the prescribed water temperature and pressure integrated into it. The supply temperature measurement is used as the condenser temperature of the water which exits the heat pump. Component 4 represents the mass flow controller, which determines the value of water flow in the building system. This component supplies the constant mass flow rate measurement to Component 5, which represents the circulation pump of the building heating system. The electric power of the circulation pump is calculated based on the default pump curve present in the Buildings library according to Equation (1). Component 6 represents the water circulation within the HVAC systems of the building. The water mass flow rate from the circulation pump is supplied to Component 7, which represents the heat pump of the building.

$$P_{el,pump} = \frac{\frac{\dot{m}_{HP}}{\rho_w} \cdot \Delta p}{\eta_{hydraulic} \cdot \eta_{motor}}, \tag{1}$$

The nominal parameters of the heat pump model, which are used for the initialisation of the simulation, are provided in Table 2. The maximum heat flow of the heat pump model wis equal to 5.8 kW for the 14 new buildings and 10.2 kW for one new building.

Table 2: Heat pump Modelica parameters.

Parameter	Value	[Unit]
Evaporator temperature difference (outlet-inlet)	-3	[K]
Condenser temperature difference (outlet-inlet)	7	[K]
District system temperature difference	3	[K]
Nominal pressure difference over condenser and evaporator heat exchanger	30 000	[Pa]
Carnot efficiency	0.5	-

The heating power is calculated using Equation (2), while the electric power required for the heat pump operation is determined with Equation (3). The COP of the heat pump is obtained with Equation (4), where η_{carnot} is a fixed value.

$$\dot{Q}_{HP} = c_{p,w} \cdot \dot{m}_{HP} \cdot \Delta T_{cond} \tag{2}$$

$$P_{el} = \frac{\dot{Q}_{HP}}{COP} \tag{3}$$

$$COP = \eta_{carnot} \cdot \frac{T_{evaporator}}{T_{condenser} - T_{evaporator}} = \frac{\dot{Q}_{HP}}{P_{el}} \tag{4}$$

Components 8 to 13 represent the connection of the district heating system to the substation. Component 8 represent the temperature sensors, which registered the temperature of the brine entering and leaving the evaporator. Component 9 represent the circulation pump transporting the brine from the evaporator loop of the demand side to the evaporator. The mass flow of the brine in this component is calculated using Equation (5). The electric power of this component is determined according to the default pump curve presented in the Buildings Library.

$$m_{br} = \frac{Q_{evap}}{c_{p,br} \cdot \Delta T_{evap,nom}} \tag{5}$$

Component 10 is utilised to split the brine flow. Component 11 is used to provide brine mass flow from the district network to the evaporator loop of the demand side, which is calculated using Equation (6). Components 9 and 10 are split, as the evaporator might operate at the temperature, which is different from the district heating network. The electric power of this component is also calculated according to the default pump curve presented in the Buildings library.

$$m_{br,DH} = \frac{Q_{evap}}{c_{p,br} \cdot \Delta T_{DH,nominal}} \tag{6}$$

Component 12 represents the delays in the thermal response of the substation to changes in the district heating fluid temperature. Component 13 represents the fluid connection of the substation to the district heating system and transfers the fluid properties to and from the distribution pipes. Component 14 calculates the total heating energy use of the building. Two parameters are used in this process – the heating power of the heat pump, calculated in the model, and the electric power of the auxiliary heater, obtained from the original data. It was assumed that the electric heater power was fully converted into heating power without any losses. Component 15 calculates the total electric power of the substation. It considers the auxiliary heater power obtained from the original data, the electric power of the heat pump, the building circulation pump's electric power, and the electric power of two district heating side circulation pumps, which are all obtained from the model. Equation (7) is used for the calculation of the total electric power of each substation.

$$P_{el}^{substation} = P_{el}^{circulation\ pump} + P_{el}^{comp} + P_{el}^{auxilliary\ heater} + P_{el}^{circulation\ pump\ at\ the\ source\ side} \tag{7}$$

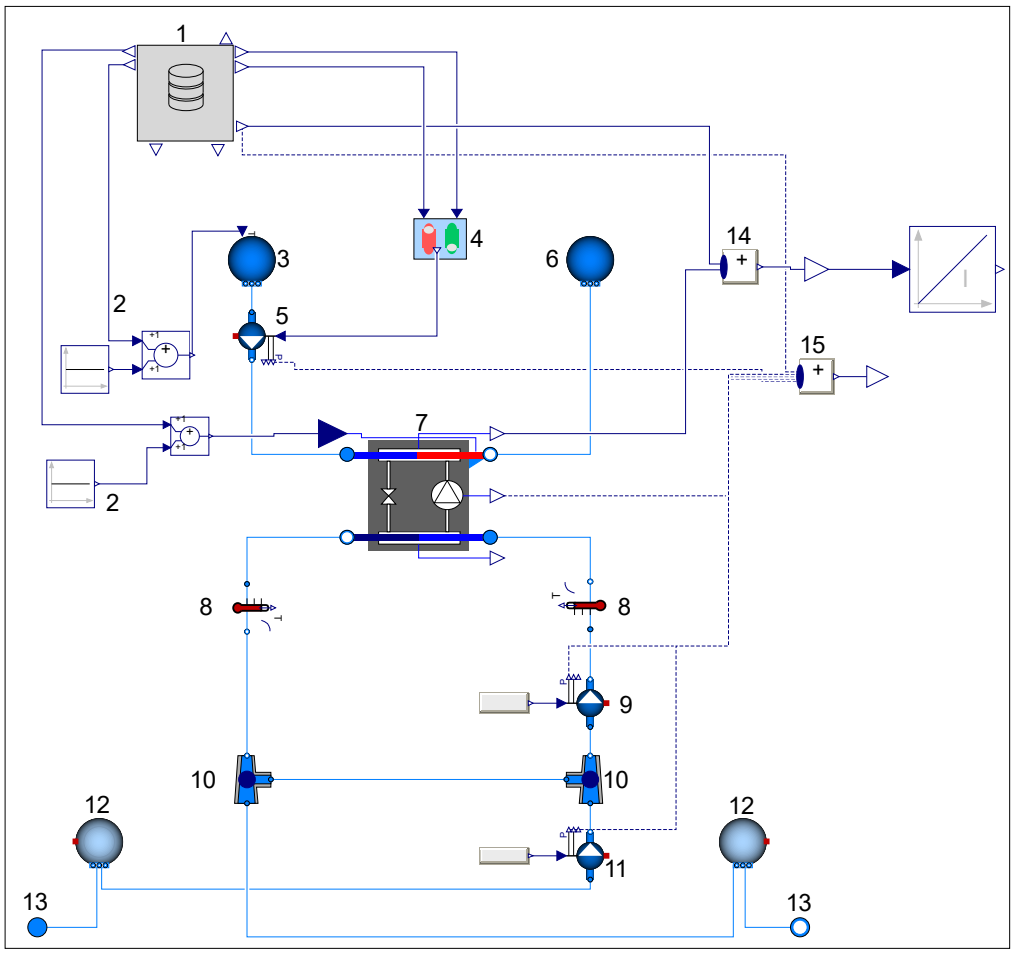

Figure 4: Modelica substation representation.

2.2.2 Uninsulated pipes model

The pipe model in this study is intended to consider the influence of pipes on each other and the heat exchange between the pipes and the ground. The calculation of heat losses/gains in the pipes is based on the (Swedish Institute for Standards, 2019) and the multipole method described in (Wallentén, 1991). This method involves calculation of the thermal interaction between the pipes and the ground separately. The first calculation considers the interaction between the pipes and the ground without considering their interaction with each other, referred to as a superposition of symmetrical problem. The second calculation focuses on the interaction between the pipes themselves, disregarding the influence of the ground, known as the anti-symmetrical problem. The visual representation of the method and the equivalent resistance model used for the calculation is provided in Figure 5. The equivalent resistance model was adapted from (van der Heijde et al., 2017). The Modelica implementation of the uninsulated twin pipes model was adopted (Abugabbara, Javed, et al., 2022) and is shown in Figure 6. The pipe boundary conditions used in the model are provided in Table 3. The values in the table are based on the thermal response test performed on-site and data from the system (*Dataindsamling fra danske termonet (HO5)*, 2022).

Table 3: Pipes boundary conditions.

Parameter	Value	Unit
Depth	1	[m]
Soil thermal conductivity	2.36	[W/(m·K)]
Soil specific heat capacity	900	[J/(kg·K)]
Soil density	1 500	[kg/m^3]
Horizontal distance between the pipes	1	[m]
Pipes burial depth	1	[m]
Mean annual surface temperature	9.34	[°C]
Surface temperature amplitude	16	[°C]
Phase lag of surface temperature	155	[days]

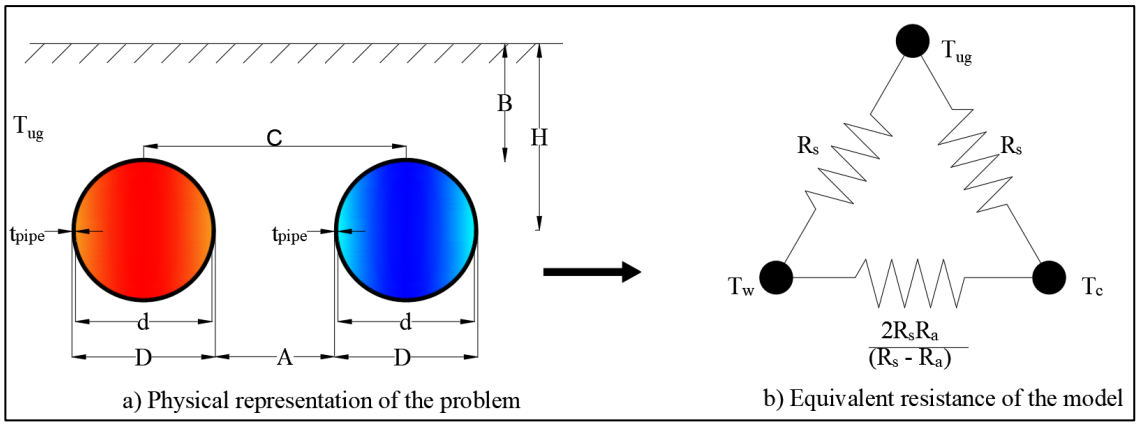

Figure 5: Physical representation of symmetrical and anti-symmetrical problem (a), and the equivalent resistance model describing this model (b).

The symmetrical resistance is calculated using Equation (8) and the anti-symmetrical resistance is calculated using Equation (9).

$$R_s = \frac{1}{2 \cdot \pi \cdot \lambda_{soil}} \cdot \left[ln\left(\frac{4 \cdot H_0}{D}\right) + \beta + ln\left(\sqrt{1 + \left(\frac{2 \cdot H_0}{C}\right)^2}\right)\right] \quad (8)$$

$$R_a = \frac{1}{2 \cdot \pi \cdot \lambda_{soil}} \cdot \left[ln\left(\frac{4 \cdot H_0}{D}\right) + \beta - ln\left(\sqrt{1 + \left(\frac{2 \cdot H_0}{C}\right)^2}\right)\right] \quad (9)$$

In these Equations, λ_{soil} is the soil thermal conductivity, H_0 is the depth with the consideration of the ground surface resistance, calculated as $H_0 = H + R_0 \cdot \lambda_{soil}$, D is the pipe outer diameter, and β is the dimensionless resistance parameter, calculated according to Equation (10).

$$\beta = ln\left(\frac{D}{d}\right) \cdot \frac{\lambda_{soil}}{\lambda_{pipe}} \quad (10)$$

The undisturbed ground temperature at depth B is calculated according to Equation (11) based on the ASHRAE guidelines (ASHRAE, 2013).

$$T_{UG,B} = T_{am} + A_s e^{-B\sqrt{\frac{\pi}{\alpha \cdot \tau}}} \cdot sin\left(\frac{2\pi \cdot (t - p_{lag}}{\tau} - B\sqrt{\frac{\pi}{\alpha \cdot \tau}}\right) \quad (11)$$

In this Equation, T_{am} corresponds to the mean annual surface temperature, A_s is a surface temperature amplitude, B is the burying depth of the pipes, from the surface level to the top of the pipe, τ is the annual period length, t is the calculation timestep (in the context of this study – one hour), and p_{lag} is the phase lag of the soil temperature.

The resulting heat losses or gains from the supply and return pipe are calculated according to Equation (12).

$$\dot{Q}_{gain/loss} = \left[\frac{1}{R_s} \cdot \left(T_{\frac{w}{c}} - T_{UG}\right) + \frac{R_s - R_a}{2 \cdot R_s \cdot R_a} \cdot (T_{\frac{w}{c}} - T_{\frac{c}{w}})\right] \quad (12)$$

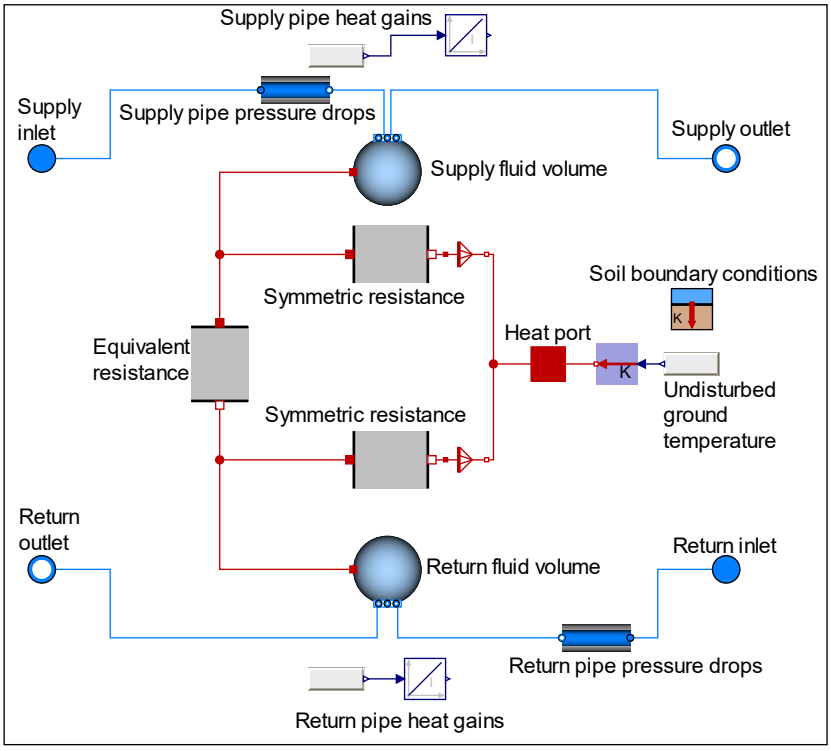

Figure 6: Diagram of the uninsulated pipe model, adopted from (Abugabbara, et al., 2022).

Equation (13) shows the relationship between the mass flow rate and the pressure drop from a hydraulic perspective. In this Equation, k is the fixed flow resistance, which depends on the nominal values. At first, this

parameter is determined using nominal values, then used in the dynamic simulation to determine the pressure drops at every time.

$$\dot{m}_{pipe} = k\sqrt{\Delta p_{pipe}} \tag{13}$$

The nominal pressure drop is calculated according to Equation (14). In this Equation, *F* is the factor, which includes the pressure losses on pipe fittings, and γ is the pipe wall friction, which depends on the Reynolds number and the roughness of the pipe. Given that the pipe is plastic, the nominal velocity was assumed to be 1 m/s and the roughness was assumed to be $2.5e^{-5}$ m (Qiao & Kajbaf Nezhad, 2021).

$$\Delta p_{nom} = F \cdot K_2 \cdot \gamma\,(Re, e) \tag{14}$$

The constant *K2* is used to consider the pipe geometry and the fluid properties and is calculated according to Equation (15). In this Equation, L is the length of one pipe segment, μ is the fluid dynamic viscosity, d is the pipe's inner diameter, and ρ is the density of the fluid.

$$K_2 = \frac{L \cdot \mu^2}{2 \cdot d^3 \cdot \rho} \tag{15}$$

2.2.3 Bore field model

The bore field model employed in this study is a derivative of the initial Modelica implementation developed by Picard & Helsen, (2014) and subsequent advancements detailed in the work of Laferrière et al., (2020). It is possible to simulate any configuration of the boreholes with the consideration of the short-term, which can occur within minutes to hours, and long-term thermal responses, which can occur at the scale from week to months. The short-term thermal response is related to the fluid transfer through the borehole and heat exchange through the filling material, while the long-term response considers the interaction between the boreholes themselves. All boreholes are connected in parallel and have the same dimensions. The properties of the boreholes and bore field configuration are provided in Table 4, and the properties of the soil remained consistent with the parameters outlined in Table 3 from Section 2.2.2. The borehole parameters were obtained from the thermal response test performed on-site.

The thermal resistance calculations of the boreholes, which are used in the borehole model, are described in (Bauer et al., 2011). The ground model uses the load aggregation method to reduce the computational requirements for the simulations, proposed by (Claesson et al., 2012) and adjusted by (Laferrière et al., 2020) to allow the implementation of different time steps. Adjusting the bore field temperature response provides the relation between the borehole wall temperature at a specific time and the heat extraction and injection rates at all preceding times. The concept of this relation was introduced by (Eskilson, 1987), and its Modelica implementation was developed by (Cimmino et al., 2014) and modified by (Cimmino, 2018). A correction of the response calculation was implemented by (M. Li et al., 2014). The model structure of the bore field is provided in Figure 7. The equations used in this model are fully described in (Abugabbara, et al., 2022). The hydraulic performance of the bore field was simulated as a function of mass flow rate.

Table 4: Borehole properties

Parameter	Value	Unit
Borehole configuration	Single U-tube	-
Number of boreholes	6	-
Thermal conductivity of the borehole filling material	1.8	[W/(m·K)]
Specific heat capacity of the borehole filling material	450	[J/(kg·K)]
Density of the borehole filling material	1680	[kg/m^3]
Borehole thermal resistance	0.12	[m^2·K/W]
Total length of the borehole	120	[m]
The radius of the borehole	0.075	[m]
Borehole buried depth	5	[m]

Parameter	Value	Unit
Outer radius of the tubes	0.02	[m]
Thermal conductivity of the tube	0.4	[W/(m·K)]
Tube thickness	0.002	[m]
Shank spacing, defined as the distance between the centre of the borehole and the centre of the pipe	0.05	[m]
Initial undisturbed ground temperature	8.7	°C

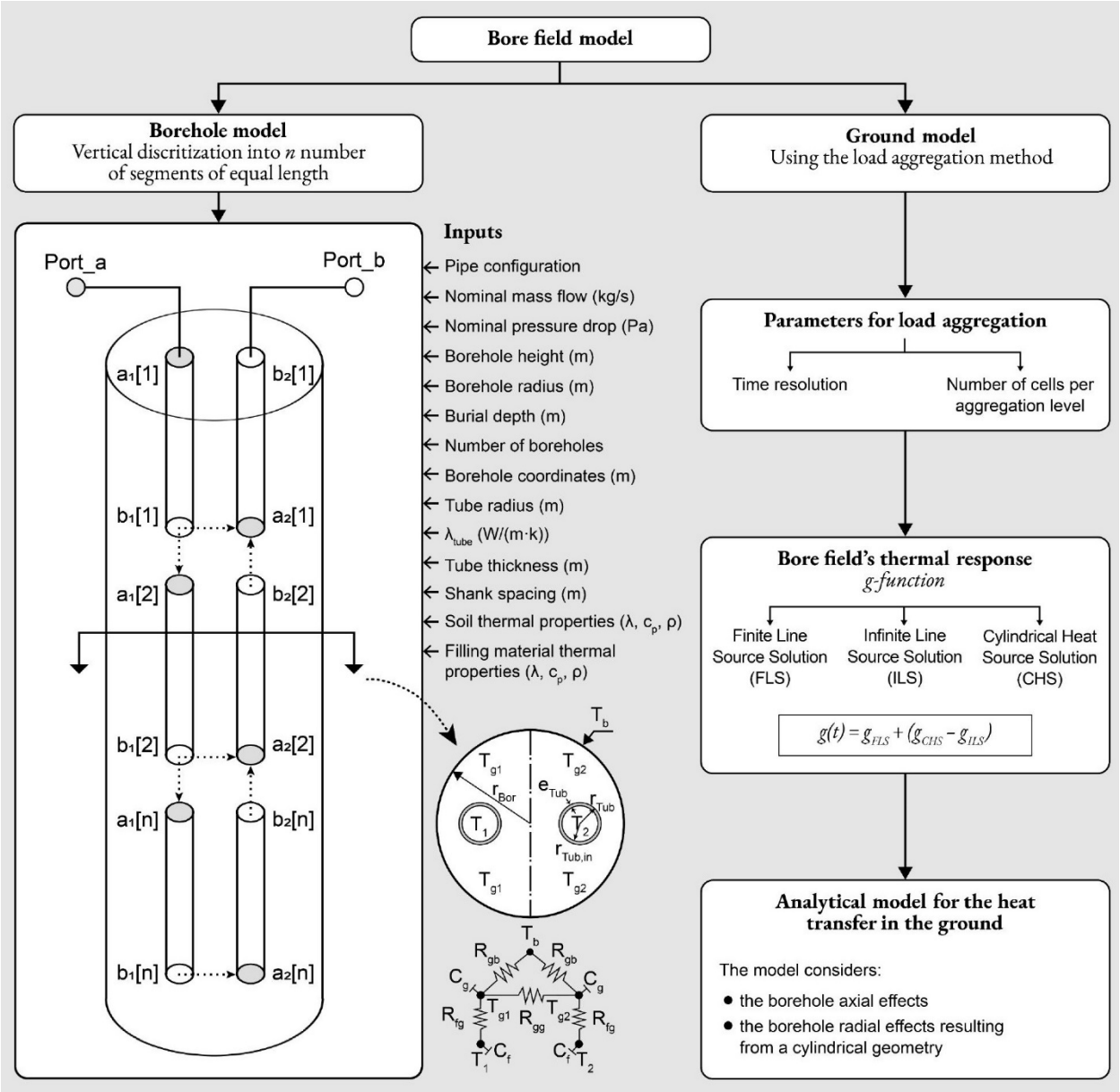

Figure 7: Bore field model structure. The model represents the borehole configuration as a single U-tube, where heat extraction occurs with a flow from port a to port b. The Figure was adopted from (Abugabbara et al., 2022).

2.2.4 Economic analysis

The Life Cycle Cost (LCC) calculation was based entirely on the existing economic analysis developed before the project implementation. The parameters and values used for the calculation can be found in Table A in Appendix. It is important to note that the existing economic analysis was conducted in 2018 before the system was installed. Therefore, today's values might differ due to the various socioeconomic factors affecting economic calculation. Nevertheless, this analysis serves as a basis for preliminary decision-making on the planning phase of the new project.

LCC calculation considered 20 years of system use, with simulated energy use calculations. Net Present Value (NPV) served as the primary value considered in the calculation. NPV was calculated based on Equation (16). *N* in the Equation corresponds to the number of life cycle years, *t* corresponds to the payment period, and *i* corresponds to a discount rate.

$$NPV = \sum_{t=1}^{N} \frac{Contribution\ margin}{(1+i)^t} \tag{16}$$

The contribution margin was calculated according to Equation (17).

$$Contribution\ margin = Revenue - Costs \tag{17}$$

The revenue was calculated according to Equation (18). The revenue included varying heating prices, heat meter prices, facility contribution prices and a fixed heating fee, which depends on the heated floor area of the building. The value is positive since the heat is generated through the analysed system.

$$Revenue = Price_h \cdot E_h + (Price_{h,meter} + Price_{Contibution}^{Facility} + Fee_{heating}^{fixed} \cdot Area) \cdot N_{buildings} \tag{18}$$

The costs were calculated according to Equation (19). They included constant prices of electricity, prices of wiring and water treatment on the demand side, administrative, service and maintenance costs of the substations and financing of the investments.

$$\begin{aligned} Costs = Price_{el} \cdot E_{el} + +(Price_{wiring} + Price_w^{treatment}) \cdot E_h + N_{buildings} \cdot (Costs_{adm} \\ + Costs_{service} + Costs_{maintenance)} + Investment_{financing} \end{aligned} \tag{19}$$

Financing of the investment was calculated according to Equation (20). This value included costs of borehole drilling, electric units, cables, renting of the heat meters, new connection pipes, earthworks necessary to install the system, wiring of the electrical units, regular and increased investment contributions, connection pipes contribution and development allowance. Financing the loan necessary for installing the system was also included in the calculation.

$$\begin{aligned} Investment_{financing} \\ = (Costs_{boreholes}^{drilling} \cdot N_{boreholes} + N_{buildings} \\ \cdot \big(Costs_{HP} + Costs_{el,units} + Costs_{cables} + Costs_{h,meter}^{rent} + Costs_{contribution}^{connection\ pipes} \\ + Costs_{contribution}^{investment} + Costs_{contribution,increased}^{investment} + Costs^{connection\ pipes}\big) \\ + Costs_{earthworks} + Costs_{wiring} + Costs_{allowance}^{development}) \cdot \left[\frac{i_{loan} \cdot (1+i_{loan})^N}{(1+i_{loan})^N - 1}\right] \end{aligned} \tag{20}$$

2.2.5 Environmental analysis

A Life Cycle Assessment (LCA) is performed for the system energy use for the B6 boundary. Due to the components' complexity, only the Global Warming Potential (GWP) is used to assess the system's environmental impact. The parameters used for the LCA calculation are provided in Table 5. The data for electricity emissions were obtained from (Egebo & Thyregod, 2022), and the data for heating emissions was obtained from (International Energy Agency, 2023).

Table 5: Environmental analysis parameters

Parameter	Value	Unit	Symbol
Number of life cycle years	20	[years]	nYea
Electricity carbon dioxide emissions (CO_2)	133	[g/kWh]	CO_2e
Electricity carbon monoxide emissions (CO)	0.17	[g/kWh]	COe
Electricity non-methane volatile organic compound emissions (NMVOC)	0.02	[g/kWh]	NMVOCe
Electricity methane emissions (CH_4)	0.09	[g/kWh]	CH_4e

Parameter	Value	Unit	Symbol
Electricity nitrous oxide emissions (N_2O)	0.003	[g/kWh]	N_2Oe
Heating GWP emissions ($kgCO_2$-eq)	41.3	[g/kWh]	GWP_h

All emissions were converted into $kgCO_2$-eq to conduct the calculations of the GWP. The methodology used for the conversion was described in (Green Delta, 2015). Therefore, first, the electricity emissions were converted to the GWP value according to Equation (21):

$$GWP_{val} = \frac{(CO_2e \cdot 1 + CH_4e \cdot 25 + N_2Oe \cdot 298 + COe \cdot 1 + NMVOCe \cdot 0.045)}{1000} \quad (21)$$

Then the GWP was calculated for 20 years for the annual energy use, based on Equation (22). The district heating emissions were subtracted from the electricity emissions, as the hot water is produced locally in the heat pump through electricity use.

$$GWP_{per} = GWP_{val} \cdot \frac{E_e}{3\,600\,000} - GWP_h \cdot \frac{E_h}{3\,600\,000\,000} \quad (22)$$

The total GWP was calculated as the sum of GWP for all 20 years.

2.3 Data pre-processing

The data retrieved from the heat pump sensors was stored in the NoSQL form (Tiwari, 2011; G. Wang & Tang, 2012). The structure of the data in the original NoSQL form is shown in Table 6. Data in the provided fragment has been edited to comply with the general data protection regulation (GDPR), but the structure remained the same. The data for most buildings were presented from 2018-11-02 to 2022-11-11, with the precision of the metering time to the seconds with three decimal places. In order to generate the input files, the data was processed in Matlab –a high-level programming language and interactive environment designed specifically for numerical computation and data analysis (Bober, 2013).

Table 6: An example of the data structure.

DeviceTime	RegisterValue	RegisterName
2019-06-20 00:00:13.500	33	REG_SUPPLY_LINE
2019-06-20 00:01:20.200	3	REG_STEP
2019-06-20 00:03:06.300	32	REG_SUPPLY_LINE
2019-06-20 00:04:08.100	4	REG_BRINE_OUT
2019-06-20 00:07:27.400	17	REG_OUTDOOR_TEMPERATURE
2019-06-20 00:08:29.000	6	REG_BRINE_IN
2019-06-20 00:11:22.000	4	REG_BRINE_OUT
2019-06-20 00:12:13.000	33	REG_SUPPLY_LINE
2019-06-20 00:15:06.000	26	REG_RETURN_LINE

The measured data structure consists of three columns: DeviceTime, RegisterValue and RegisterName. The RegisterName column in this structure serves as a descriptor of the value, which is written in the RegisterValue column and associated with a specific timestamp in the DeviceTime column. For example, in the provided fragment, the system registered a change in the water supply temperature, which reached 33 °C at 00:00:13.500 on the 20th of June 2019. Every building dataset encompassed the following descriptors:

- REG_OUTDOOR_TEMPERATURE – describes the outdoor temperature measurements.
- REG_BRINE_IN – describes the brine temperature measurements of brine leaving the district heating network and coming to the heat pump. This measurement was obtained by sensor 1 in Figure 2.

- REG_BRINE_OUT – describes the brine temperature measurements of brine leaving the heat pump and coming to the district heating network. This measurement was obtained by sensor 2 in Figure 2.
- REG_SUPPLY_LINE – describes the supply temperature measurements of the water leaving the heat pump and coming to the building system. This value was measured by sensor 3 in Figure 2.
- REG_RETURN_LINE – describes the return temperature measurements of the water leaving the building system and coming to the heat pump. This value was measured by sensor 4 in Figure 2.
- REG_STEP – describes the auxiliary electric heater energy use measurement in the heat pump.

As the direct data processing of the NoSQL structure could not be performed, an algorithm was developed to reorganise the information to the relational structure. The algorithm is depicted in Figure 8. The algorithm is separated into three sections. Section one handled the conversion from NoSQL to a relational data form, the second managed the data processing, and the third generated the output data.

Initially, only the first and third sections were utilised to ascertain data patterns and define the boundaries necessary for data cleansing by extracting and outputting each data type into the .xlsx format for manual processing. The first section starts with reading the collected data from a building, presented in a .csv format. To facilitate further processing, it extracts the unique DeviceTime values (a 'time array') for the building, discounting the seconds to avoid generating irrelevant unique values. This part of the algorithm extracts outdoor temperature, brine supply and return temperatures, water supply and return temperatures, and the auxiliary power of the electric heater based on the descriptors, as shown in Table 6. The extracted measurements are referred to as "types" in the algorithm.

Subsequently, a new time array was generated, spanning a continuous period from 01:00 on 02/11/2018 to 01:00 on 11/11/2022, at a one-minute resolution. This period was selected as it contains data for most buildings, and the simulation software requires data in a continuous format. For instance, a time array containing data for the 23rd and 25th of November, but lacking data for the 24th, would be processed incorrectly by the Modelica modelling environment.

The original time array and associated measurements were then synchronised with the new time array, resulting in a new table featuring continuous time and corresponding measurements. Since measurements were not consistently taken throughout the entire period and were recorded only when parameters changed, it was necessary to fill in missing data. This step is called "processing missing values" in the algorithm. This involved implementing a conditional statement to check if values were present in the table's initial time period (01:00 on 02/11/2018). If these values were absent, they were supplemented with the first existing value of the same type. Subsequently, the algorithm's first section scanned each data type in the table, identifying missing values and filling them based on the initial value of the same type. For instance, if the brine supply temperature measurement was missing for 08:00 on 02/12/2019 but was recorded as 1 °C at 07:59 on the same day, the missing value would be filled with 1 °C. The resulting table from section 1 of the algorithm was filled with data without any gaps and produced in minute resolution.

The final processing and simulation resolution was hourly, as a minute-based resolution would place excessive computational demands. Consequently, it was necessary to retime the table created in section 1 of the algorithm to an hourly resolution. The retiming was based on the median principle: every 60-minute value for each type was added and divided by 60. The resultant table, with hourly data, was saved in a .xlsx format for manual analysis in MS Excel software. The findings from the preliminary data analysis served as the foundation for the complete data pre-processing.

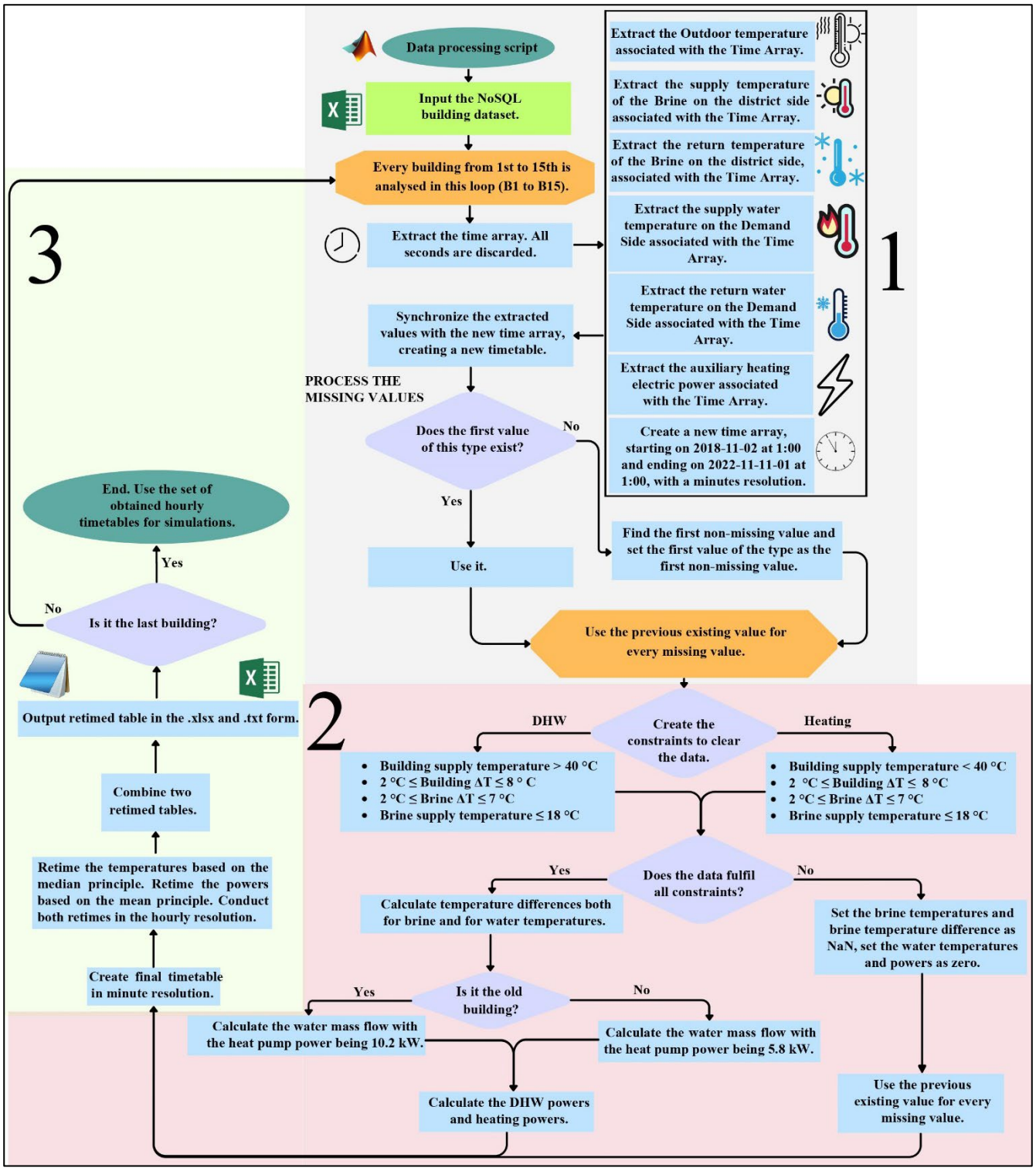

Figure 8: Data pre-processing algorithm.

Figure 9 presents the brine temperature difference boxplots for every building in the set. The whisker range of the boxplot here is equal to the 1.5 interquartile range. One observation from the Figure is the significant amount of missing data for all buildings, buildings 13 and 14 in particular, which were connected to the system in 2022. The output indicates that the brine temperature was in the range between 2 °C to 7 °C. There are also several negative brine temperature differences, which is unlikely in the analysed system since it only provides heating. This could be explained by the fact that sensors registered information only when the measured temperature changed. These sensors continued to measure the temperature when there was no brine flow, resulting in erroneous values.

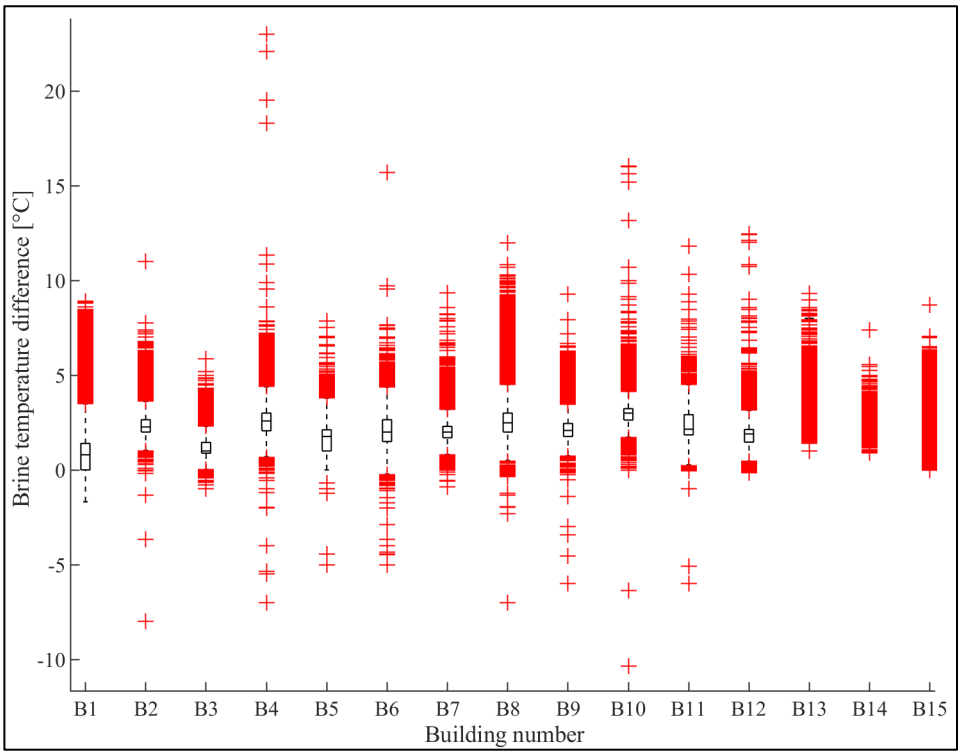

Figure 9: Brine temperature difference for all buildings.

Figure 10 presents water temperature differences plotted over the entire measurement period for all 15 buildings. The whisker range of the boxplot here is equal to the 1.5 interquartile range. The findings indicate that the water temperature difference was between 2 °C and 9 °C. These data also indicated a few incorrect data points, as the water temperature difference was also negative in some cases, which could also be explained by the way sensors measure temperature.

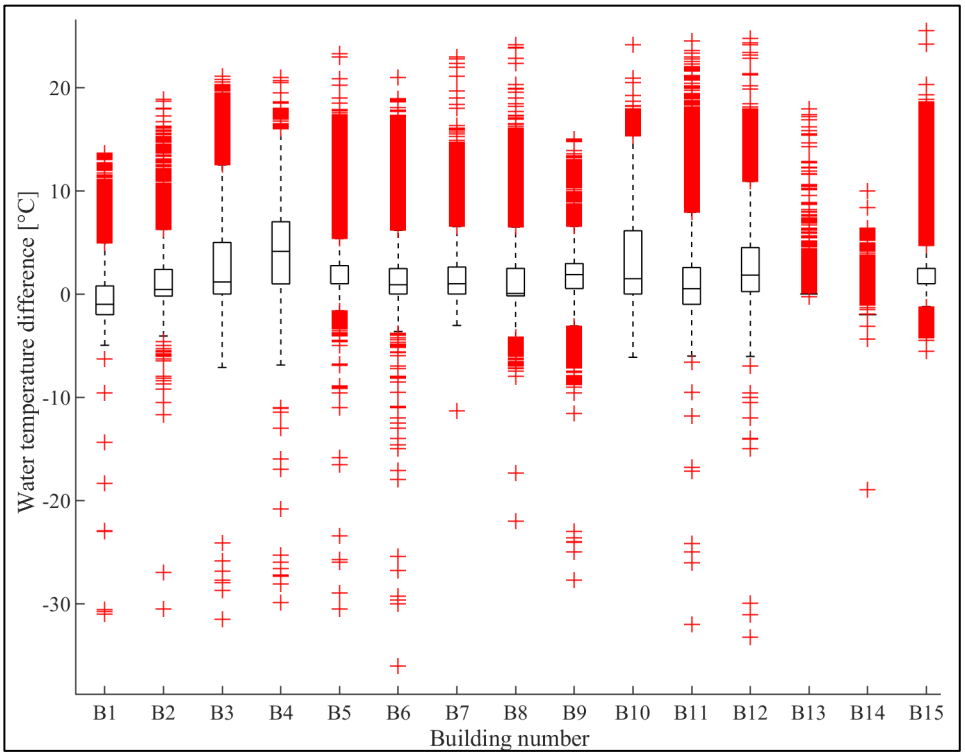

Figure 10: Water temperature difference for all buildings.

Figure 11 compares the brine supply temperature and outdoor temperature in hourly resolution. Different data series in the Figure indicate different buildings. This comparison revealed that a significant portion of the data

might be unrepresentative, as the brine temperature consistently reached 25 °C. In comparison, the soil temperature at a depth of one meter never surpasses 17 °C according to the climate data (Wang et al., 2013), which were modelled based on (Kvisgaard et al., 1980).

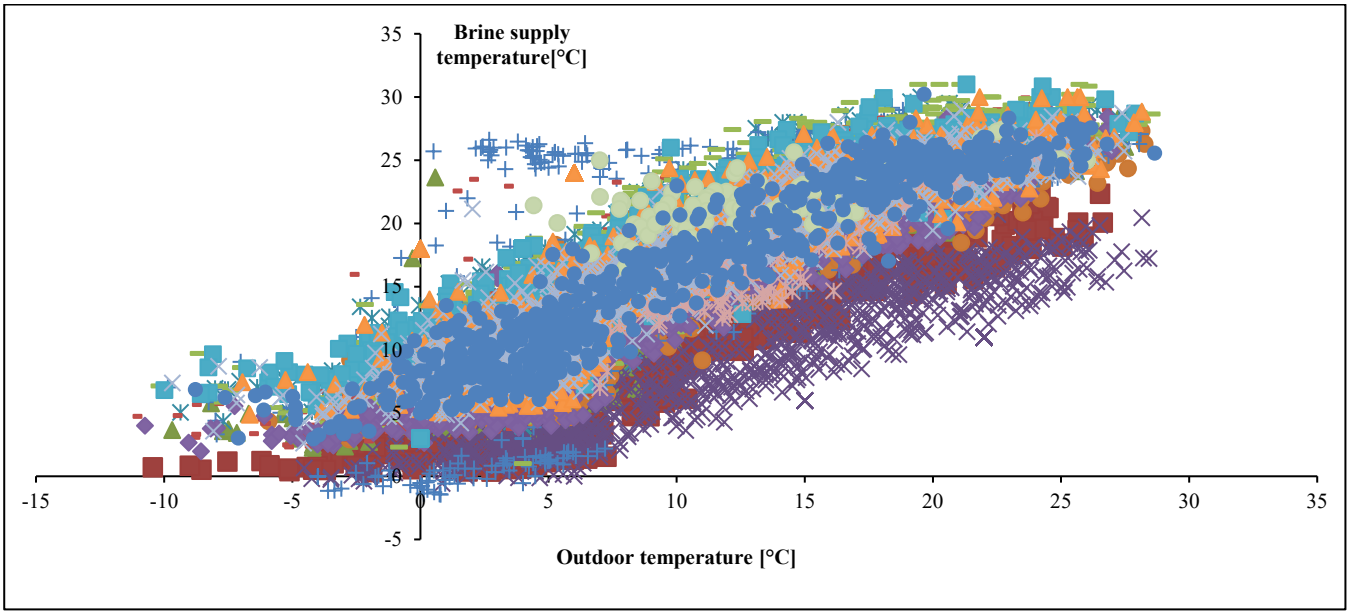

Figure 11: Relationship between the outdoor temperature and brine supply temperature.

Considering the number of outliers and unrepresentative data points, a noise-cleaning procedure was implemented by introducing the second section of the algorithm, presented in Figure 8. Once the relational data structure was created, new constraints were applied to the maximum temperature difference, limited to 8 °C for space heating and DHW production and a corresponding cap of 7 °C for brine temperature at the supply level. Another restriction was placed on the minimum temperature difference, set at 2 °C for both the system and building levels. An additional constraint was introduced to separate DHW production from heating energy consumption. DHW production was assumed to occur when the supply temperature exceeded 40 °C, while temperatures below this threshold were assumed to indicate that the substation generated was used for heating purposes. These constraints were selected based on the preliminary data processing findings, the typical heat pump operation (Liu et al., 2020), and the equipment installed in the system. A constraint of the maximum brine supply temperature of 18 °C was implemented based on the meteorological information on the soil temperature in this region of Denmark (Wang et al., 2013). It should be noted that the reference value is based on the specific soil temperature model, and this value could vary with the different climate models.

The data that fulfilled these constraints were further processed, and temperature differences were calculated for brine and water. As the system model required heating loads for the simulation, the mass flow value was required to proceed with the data pre-processing. According to previous studies of similar small-scale systems and the constant speed circulation pump installed in the system, the mass flow rate was assumed to be constant (Liu et al., 2020). The mass flow rate of the condenser was calculated according to Equation (2). The maximum temperature difference here was the same as in the constraints applied to the data. A conditional statement was implemented in the algorithm to check if the analysed building is the existing one. This statement was implemented due to a heat pump with higher capacity in the existing building. For the existing building, the maximum heat pump power was set to be 10.2 kW. In contrast, the maximum heat pump power for the new buildings was set to 5.8 kW, according to the system description (*Dataindsamling fra danske termonet (HO5)*, 2022).

Then the mass flow rate was used to calculate the actual heating power, according to Equation (23). The heating energy use was assumed to occur when the supply temperature was below 40 °C, and the DHW production was assumed to occur when the supply temperature was above 40 °C, as was stated in the system description.

$$\dot{Q}_{HP} = c_{p,w} \cdot \dot{m}_{HP} \cdot \Delta T_w \tag{23}$$

The data that did not fulfil the requirement was processed differently. The supply and return water temperatures were set to 20 °C, which is the default medium value used in the Modelica simulation. The brine supply and return temperatures were set as NaN values, and the powers were set as 0. Then the brine supply and return temperatures were processed the same way as the missing values in the first section of the algorithm. These data were also used in the creation of the final timetable.

After this processing, the final timetable was created and retimed hourly. The high uncertainty of the temperature levels in the brine was the reason for selecting the median retime principle, to avoid the outliers from influencing the values in the dataset. The median retime principle meant that for every 60 values in the minute resolution table, a median value was calculated and used for this specific hour. This uncertainty was not present in the case of powers, as they were obtained through calculation, therefore, they were retimed on the mean principle. Two outputs were generated from this processing: a .xlsx file for manual processing and a .txt file for input in the modelling software.

The outcomes of the data processing are summarised in Figure 12. The total heating load of the entire system over four years, according to the processed data, was 314.1 MWh without the consideration of the electric heater and 365.8 MWh with the consideration of the electric heater, which mostly corresponded with the predicted performance of the system, where one building uses approximately 8 MWh of heating energy per year (*Dataindsamling fra danske termonet (HO5)*, 2022), with the consideration that two buildings were connected to the system in August 2022, and one building was connected to the system in January 2020. The distribution of heating energy use between domestic hot water and heating load also exhibited similar patterns to comparable systems in the same climate conditions (Liu et al., 2020).

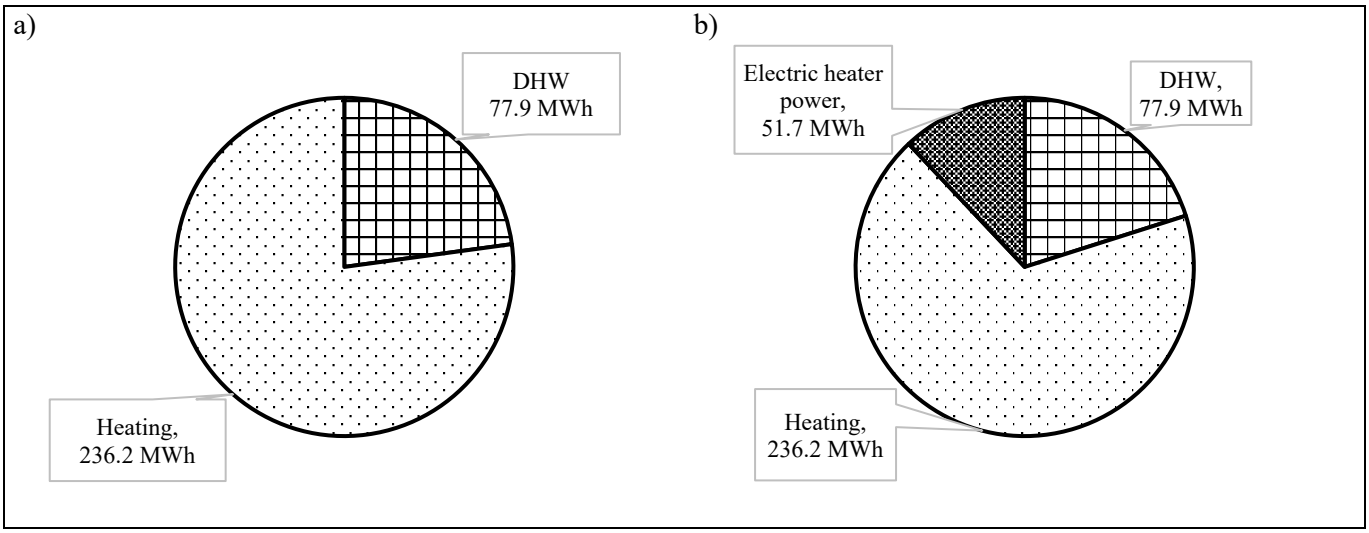

Figure 12: Analysed system energy use distribution. Figure 12a shows the thermal energy use without the electric heater, and Figure 12b presents the thermal energy use with the electric heater.

2.4 Key performance indicators (KPI)

In order to evaluate KPI, a few metrics were considered to assess different aspects of the model:

- Brine supply and brine return temperature were used to evaluate the model's validity by assessing the accuracy of the simulated temperatures compared to the measured temperatures.

- Seasonal Performance Factor (SPF) was utilised to assess the technical efficiency of the system, demonstrating the ratio of heat output to energy input over a season and highlighting the system's effectiveness in converting energy to useful heat. Equation (24) was used to calculate SPF, considering the total heating and electric energy supplied to the system. This calculation considered the energy outputs from each substation for all buildings in the system.

$$SPF = \sum_{\text{Building 1}}^{\text{Building 15}} \frac{E_h}{E_e} \quad (24)$$

- Net Present Value (NPV) was used to assess the system's economic performance, considering the initial investment, operating costs, and potential revenues. A higher NPV indicates a more favourable economic return on investment.

- Global Warming Potential (GWP) was used to evaluate the environmental impact of the system, measuring the amount of greenhouse gas emissions associated with the system's operation and comparing it to the emission of CO_2 as the reference gas. Lower GWP values signify reduced environmental impact.

- Heat gains/losses in supply and return pipes were used for the technical evaluation of the model, examining the efficiency of the piping system and its ability to minimise heat losses or maximise heat gains during transmission between the district heating system and the building substations.

2.5 Model validation

According to the (ASHRAE, 2017), two metrics were used to evaluate the validity of the model – normalised mean bias error (NMBE), calculated according to Equation (25) and cross variance of the Root Mean Square Error (CV(RMSE)), based on Equation (26). Brine supply and return temperatures were selected as the values, which were compared between the model and the original data. According to the ASHRAE guidelines, NMBE should be within the range of -10% to 10%, and the CV(RMSE) should be within the range of -30% to 30% for the model to be considered valid. Only specific periods were validated in this case due to considerable uncertainty within the measured data. Therefore, only the winter hours, which had the brine temperature within the range of 2 °C to 6 °C, with a water supply temperature of at least 30 °C where the data existed for at least 50 minutes, were considered for the validation. Two buildings were excluded entirely from the evaluation, as they only have the data from August 2022 to November 2022.

$$NMBE = \frac{1}{T_{mean,measured}} \cdot \frac{\sum_{i=1}^{n}(T_{measured} - T_{modelled})}{n-1} \quad [\%] \quad (25)$$

$$CV(RMSE) = \frac{1}{T_{mean,measured}} \cdot \sqrt{\frac{\sum_{i=1}^{n}(T_{measured} - T_{modelled})^2}{n-1}} \quad [\%] \quad (26)$$

These metrics provide a basis for evaluating the accuracy and validity of the model by comparing the measured and modelled values of brine supply and return temperatures. The model can be considered valid for the selected periods if the NMBE and CV(RMSE) values fall within the specified ranges.

2.6 Limitations

The study has several limitations that should be considered when interpreting the results:

- Uncertainty of sensor data: The lack of data considering the actual placement of sensors and potential influencing factors introduce uncertainty in the results. Furthermore, the original data was provided in varying time resolutions, leading to data processing challenges. Accurate sensor placement and consistent data resolution would improve the data quality and increase the results' reliability.

- Missing data: Across all the buildings which were connected to the analysed system from the start, 49.68 % of data was erroneous. This increases the likelihood of errors in the results and may limit the ability to draw accurate conclusions from the findings. Addressing the missing data issue in future research would help enhance the reliability and validity of the results.

- LCA limitation: The system's complexity made a complete analysis of its environmental impact unfeasible. Consequently, the final result of the analysis may significantly differ from what is obtained in this research. A comprehensive LCA would provide a more accurate environmental impact assessment and lead to more informed conclusions about the system's performance.

- Input sensitivity: The model used a lot of different input values. The sensitivity of these values was not analysed, meaning that even the slightest change in one of the inputs could strongly influence the results.

- The economic analysis used the data from 2018, which did not consider several socioeconomic and political changes which happened since that year. However, it can still be used for the preliminary economic assessment.

- Much of the data depended on the inputs, for example, the hydraulics part of the calculation. Therefore it is possible to assess the system's potential in some cases but not its actual performance.

3 Results

The simulation results serve as the foundation for a comprehensive analysis of the analysed district heating system, evaluating its performance in terms of energy use, efficiency, heat losses, and environmental impact. This section presents the findings derived from the model, considering the various aspects and components of the system.

3.1 Model validation

The results of the model verification are demonstrated in Table 7. As can be seen from the results, the model demonstrates a high degree of similarity between the original data and the modelled data for the specific periods, where the data was correct with a high confidence. The positive value of NMBE means that the temperature is higher in the model compared to the measurement. In contrast, the negative value of NMBE means that the temperature is lower in the model compared to the measurement. Higher absolute values of NMBE and CV(RMSE) mean a higher difference between the model and the measurement. The supply brine temperatures demonstrate much higher variability in NMBE and the CV (RMSE) due to the temperatures in these periods being close to zero, leading to difficulty interpreting the results, as the Equations include mean measured temperatures in the denominator. The error might be overestimated if these values are close to zero.

Table 7: Validation results

	Brine supply		**Brine return**	
	MNBE	**CV(RMSE)**	**MNBE**	**CV(RMSE)**
B1	1,42	27,20	-0,21	-9,49
B2	-1,46	16,82	-0,95	-8,97
B3	0,66	-12,98	-0,16	-8,06
B4	0,71	10,78	-0,49	-14,40
B5	-0,27	-11,35	0,09	-7,54
B6	0,99	18,32	-0,07	-9,50
B7	-0,72	-14,95	0,40	-8,09
B8	-0,09	-7,42	0,32	-7,03
B9	0,73	-8,40	-0,47	-7,33
B10	-0,17	26,92	-0,10	-9,57
B11	-1,23	-16,34	0,11	-8,09
B12	-0,23	-19,47	-0,86	-8,51
B15	11,67	19,13	0,61	-10,18

3.2 System analysis

Figure 13 presents the energy balance of the assessed low-temperature district heating system, covering the period from 2018-11-02 01:00 to 2022-11-11 01:00. The Figure illustrates the heating energy use (including both space heating and domestic hot water loads), electric energy use, and piping losses separately for supply and return pipes. It is important to note that the modelled energy use is higher than the value obtained from data processing; however, it aligns with measured data, which indicates an average energy use of 10 MWh/year per building rather than the previously calculated 8 MWh/year (Dataindsamling fra danske termonet (HO5)). As expected, the losses for both the return and supply pipes are negative, suggesting that the system gains heat from the ground rather than losing it to the ground, resulting in a better performance of the analysed system. The results also show an increase in energy use coinciding with the connection of new buildings to the district heating system. This finding aligns with expectations, as additional buildings increase the overall demand for heating energy. However, it's worth mentioning that the data for 2018 and 2022 is incomplete due to a lack of data for certain months. Consequently, the analysis for these years might not be entirely representative of the system's performance during those periods.

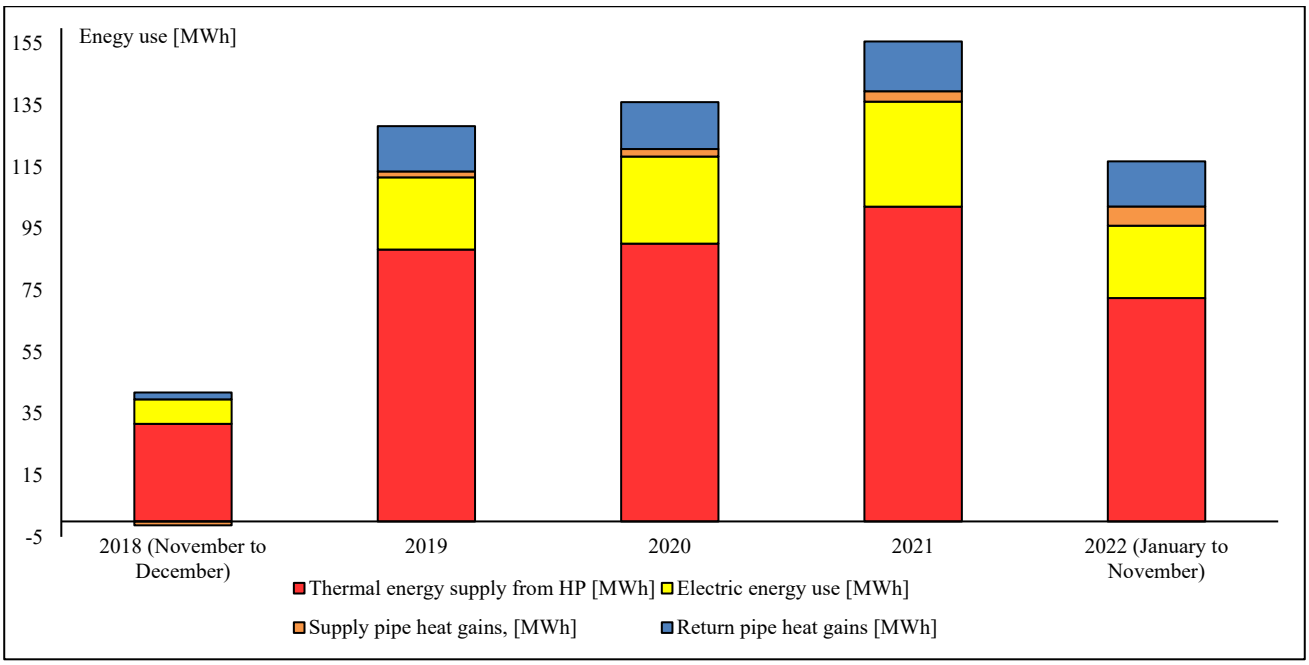

Figure 13: Energy balance of the analysed system.

Figure 14 presents a relationship between the modelled mass flow and modelled pressure drops of the bore field system based on the simulation results. The values of pressure drops correspond to the previous studies of the existing systems and measured pressure drops in the systems of similar configuration, suggesting that the simulation parameters were selected correctly (Javed et al., 2022). It can be seen from this result that the pressure drops of the system at the peak capacity are quite low, meaning that the electricity use for the circulation pumps is low as well. Lower electricity use reduces both operational costs, and the environmental impact of the system, particularly if the electricity is generated from non-renewable sources. Thus, the low-pressure drops, as seen from the results, suggest both economic and environmental advantages of the analysed LTDH system.

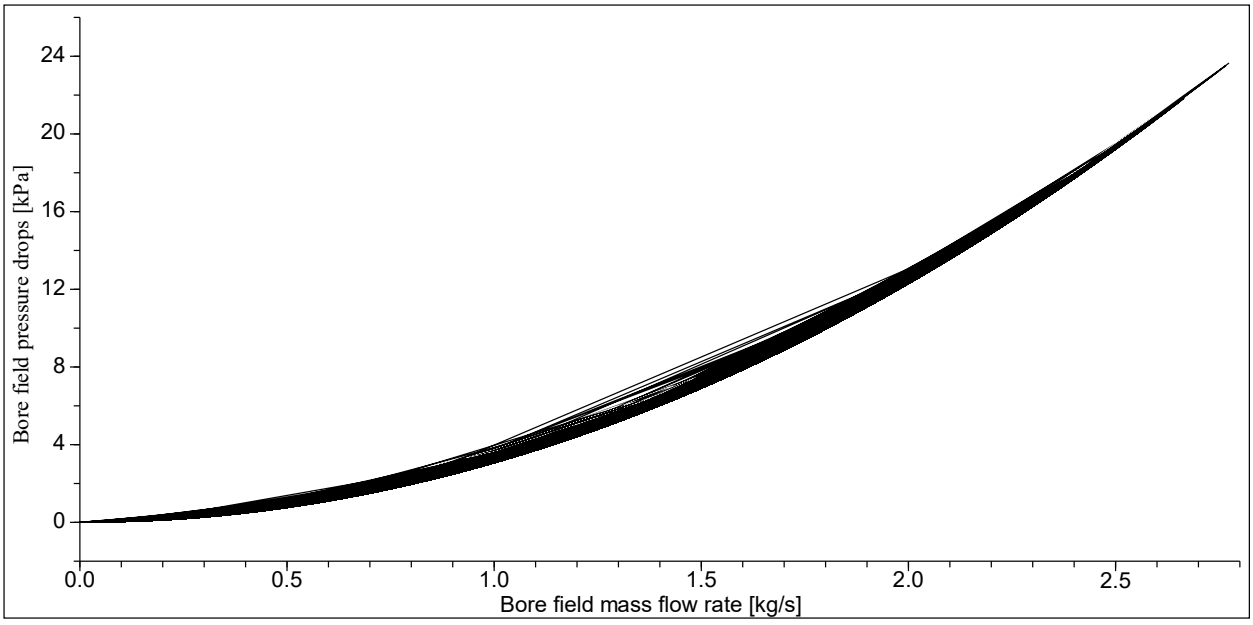

Figure 14: Relationship between the bore field mass flow rate and bore field pressure drops.

Figure 15 depicts the modelled brine bore field leaving temperature on the left axis (read line), plotted against the measured outdoor temperature on the right axis (black dotted line), with time serving as the independent variable. visual representation of the modelled brine bore field leaving temperature, displayed on the left axis, juxtaposed with the measured outdoor temperature on the right axis. Time serves as the independent variable in this analysis. The results obtained from this graph reveal a specific trend: the borehole leaving temperature

begins to exhibit a decline around the onset of 2021. This observed decrease in the bore field leaving temperature can be attributed to the particularly cold winter experienced in 2020-2021 (days 760-850), as indicated by the demonstrated outdoor temperature. It was expected that the bore field leaving temperature would be lower during this period due to the higher heat demands in this period. However, the brine temperature experiences a decrease not only during winter but also during the summer months. This observation becomes especially clear during the subsequent winter of 2021-2022 (days 1125-1815) when the outdoor temperature resembles that of winter 2019-2020 (days 394-485). The consistent decrease in brine temperature, both in summer and winter, suggests that the system is experiencing ground heat depletion. This outcome was anticipated, as the system operates solely by extracting heat from the bore field without returning any heat back into it. Consequently, over time, the ground heat available within the system diminishes, leading to the observed reduction in brine temperature.

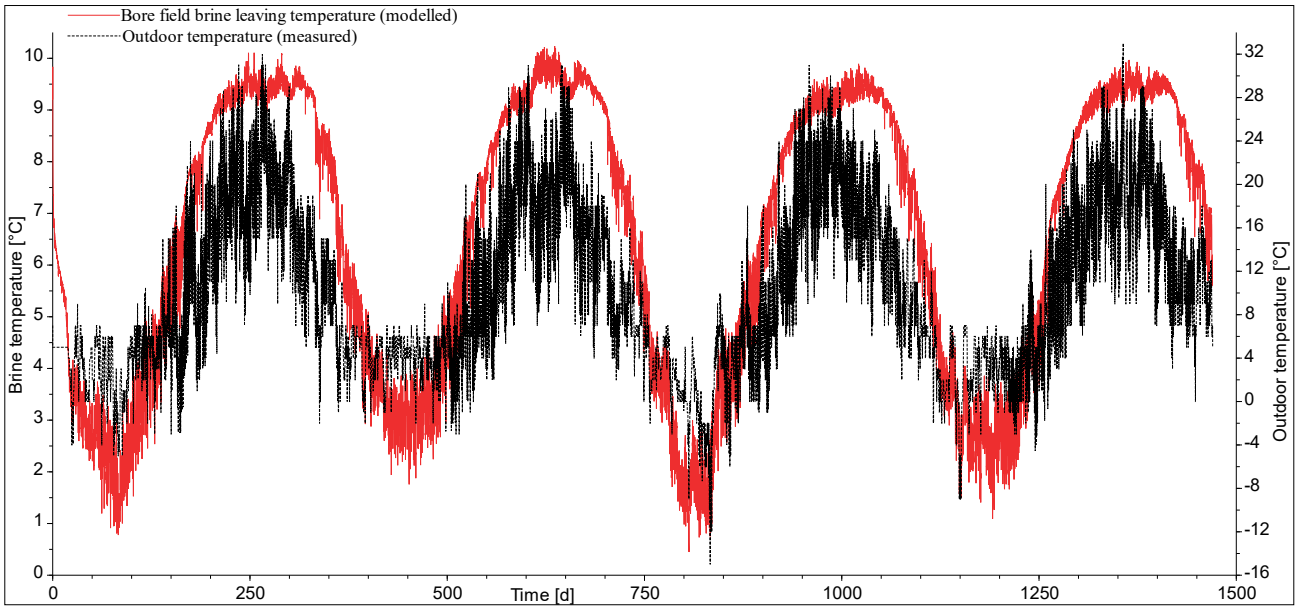

Figure 15: Borehole leaving temperature.

Figure 16 shows the comparison between the measured and simulated brine supply temperatures. The measured brine temperature is depicted using a black boxplot, while a blue boxplot represents the simulated brine temperature. In this visualization, the whisker range of the boxplot is determined to be equal to the 1.5 interquartile range. It is evident from the provided Figure that, in most cases, the measured and simulated brine supply temperatures exhibit a noticeable correlation. This observation holds true not only for the median values but also for the overall distribution of temperatures. Such close alignment between the measured and simulated data points suggests that the model accurately captures the behaviour and thermal characteristics of the system under consideration. However, it is worth noting that the data for certain buildings within the analysed district heating system lack a correlation between the measured and simulated brine supply temperatures. Buildings 13 and 14, for instance, were connected to the district heating system in 2022, and as a result, there is an insufficient number of valid data points available for these buildings. Consequently, the lack of correlation observed in these cases can be attributed to the limited data availability. Similarly, Building 15 also exhibits a lack of correlation between the measured and simulated brine supply temperatures. This discrepancy can be attributed to the fact that Building 15 was connected to the district heating system in 2020, and many data points are missing for this building. However, as 12 buildings out of 15 are pretty similar, it can be determined that the model is valid.

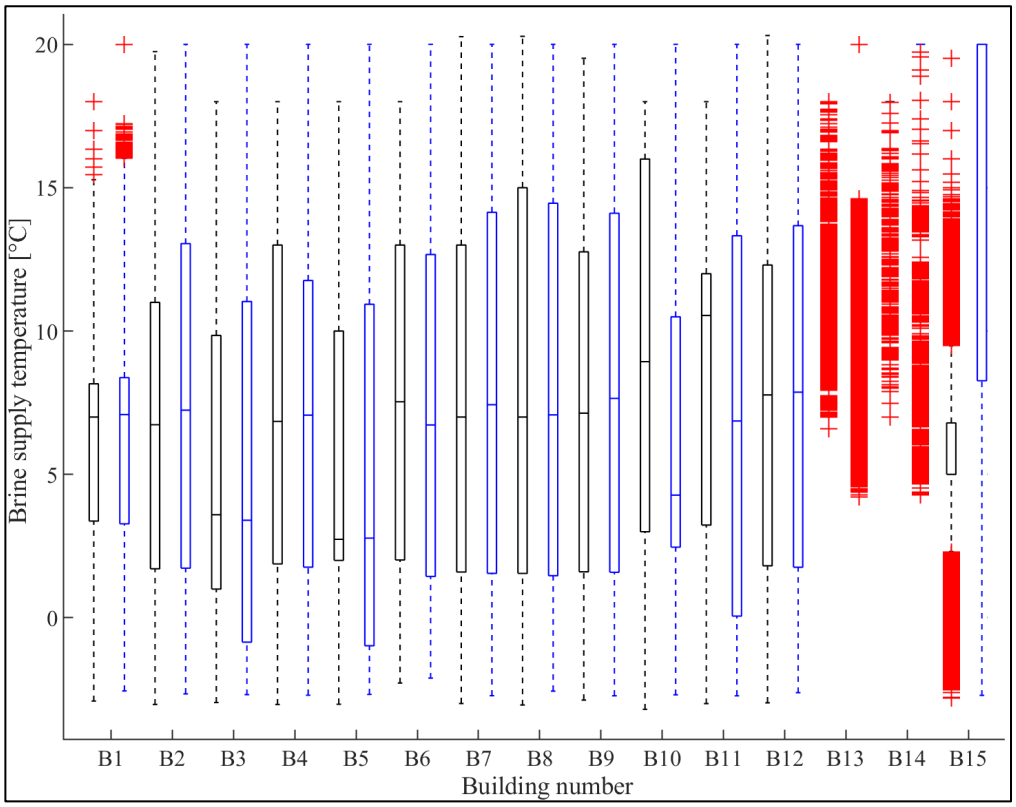

Figure 16: Comparison between the measured (black) and simulated (blue) brine supply temperature for all buildings.

Figure 17 presents the comparison between the measured and simulated brine return temperatures. The measured brine temperature is shown with a black boxplot and the simulated brine temperature with a blue boxplot. The whisker range of the boxplot here is equal to the 1.5 interquartile range. The same trend as with the supply temperature is also observed here, showing the lack of correlation only for the buildings with a considerable number of missing data.

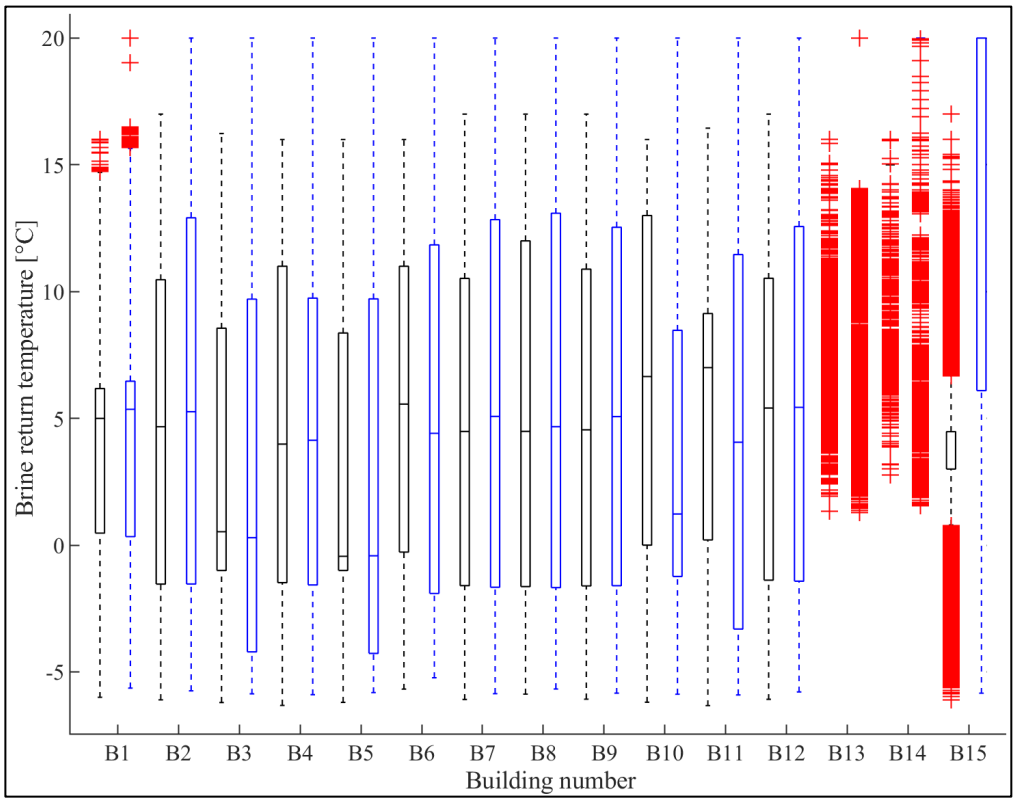

Figure 17: Comparison between the measured (black) and simulated brine return temperatures for every building.

3.3 Techno-economic and environmental analysis

Figure 18 presents the techno-economic and energy use environmental analysis outcomes for the investigated system. In this analysis, the Seasonal Performance Factor (SPF) is the independent variable depicted on the x-axis. On the y-axis, the Figure employs dual scales to demonstrate two other KPIs of the system's performance - Net Present Value (NPV) and Global Warming Potential (GWP). The NPV is plotted on the left-hand side of the axis, and it represents the economic viability of the system. GWP, plotted on the right-hand side, presents the environmental footprint of the system energy use. The trajectories of NPV and GWP are depicted in orange and green, respectively, while the red dots represent the model's actual performance. It can be seen from this result that the system's techno-economic aspect has a room for improvement, indicating that the system may not be economically profitable at the moment. However, it also implies that from an environmental perspective, the system performs positively as the total GWP of the energy use is negative.

A series of tests were conducted involving incremental changes in the SPF to determine the SPF threshold for profitability over 20 years and evaluate its impact on CO_2 emissions. This approach allowed to assess the economic potential of the analysed system. The analysis results demonstrate that increasing the SPF to approximately 3.75 leads to a turning point where the modelled system becomes profitable, accompanied by a further reduction in carbon emissions.

It should be noted that the LCC and LCA calculations were conducted for 20 years only and the prices used in this study were taken from 2018. Therefore, the true economic viability of the system might not be correctly reflected in this result. The study's environmental impact findings, represented by the Global Warming Potential (GWP), are heavily dependent on the electric energy mix in use and might vary depending on the used electrical and district heating energy mix.

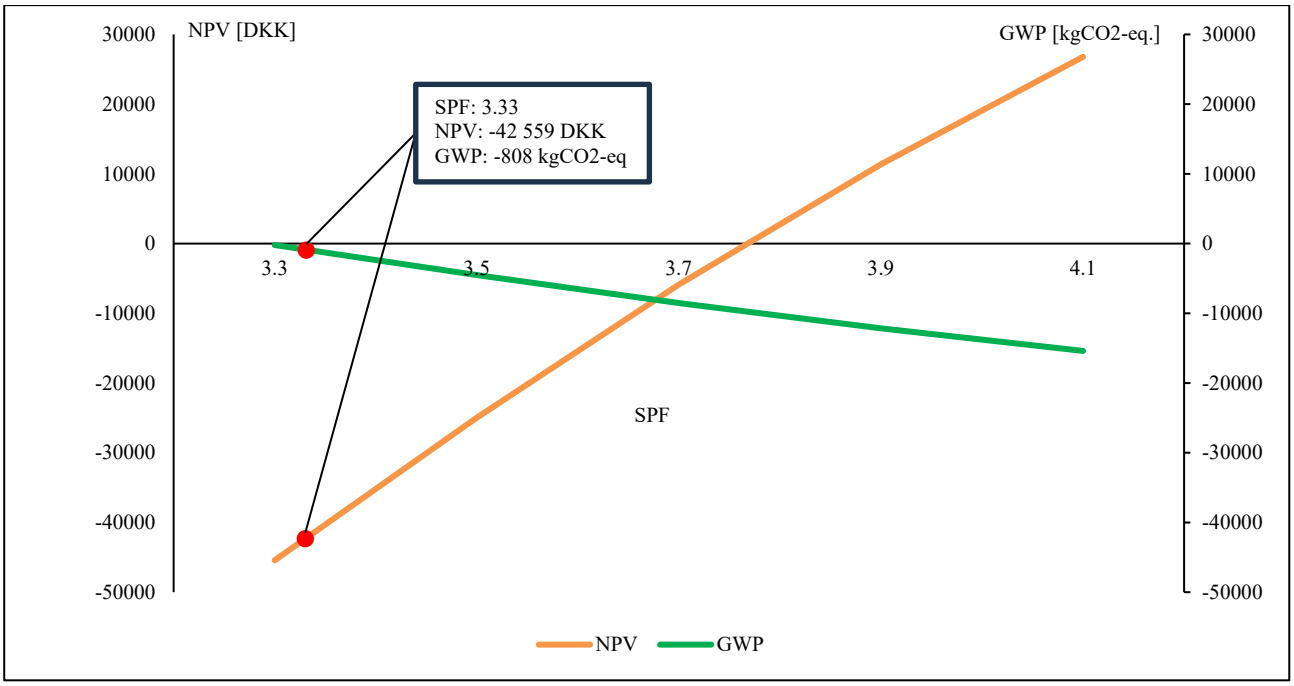

Figure 18: Seasonal performance factor (SPF) of the analysed LTDH system, and its corresponding global warming potential and net present value.

4 Discussion

The analysed low-temperature district heating system with decentralised heat pumps and the bore field thermal energy storage offers several valuable insights and conclusions. The model of the system was investigated, as the measured data did not provide much insight into the techno-economic insight of the LTDH system. The modelled system was validated, and its performance seems to align with the measured data or the previous studies. However, a few issues remain, specifically that most of the buildings have a period of missing data, which were replaced in this research with constant values. While it provides the possibility to simulate the system, it still creates uncertainty in the results. The efficiency of the data processing algorithm is also questionable due to high uncertainty of the validity of the original data. Additional sensors may need to be installed within the system to obtain higher-quality results. Although the validation metrics guarantee a certain level of validity for the results obtained, the accuracy of the measured data during summer periods remains uncertain.

The potential hydraulic performance of the modelled system seems to be pretty good, as the analysed LTDH system has low-pressure drops on the bore field level, therefore reducing the electric energy use and the amount of purchased electric energy. Nevertheless, it is a modelled value, as the hydraulic results of the existing system were not obtained.

The bore field leaving temperature compared to the outdoor temperature indicates that the system supply temperature levels are decreasing, which can be attributed to ground heat depletion. As the system works only in the heating production mode, there is no reinjection of the cold energy into the ground, which reduces potential useful energy. The low SPF value for the ground source system also supports this conclusion. One potential solution to this issue is the introduction of direct free cooling to the substations. The brine temperature will be consistently close to the ground temperature, ranging between 15°C and 17°C in the Summer. This temperature range enables the system to exclusively utilise high-temperature free cooling as its cooling method. Implementing this solution could help alleviate the problem of heat depletion in the ground while improving the overall efficiency and performance of the district heating system. Additionally, global warming can cause overheating in the new energy-efficient buildings and renovated buildings (Li et al., 2012; Marsh et al., 2009; Psomas et al., 2016), which could also be solved by the free cooling, thus boosting the climate resilience of the analysed LTDH system.

Another aspect to consider in relation to brine temperature is the impact of uninsulated pipes on temperature quality. At present, the piping of the analysed LTDH system is working as a long horizontal ground heat exchanger. The additional heat gains increase the brine temperature on the supply side, thereby offering the opportunity to extract more heat from the fluid. However, if the system were to be designed to combine district heating and cooling, which is common for low-temperature systems, the fluid's temperature quality during summer would decrease.

From an economic standpoint, the system's performance appears to be unfavourable with the current efficiency. Two main factors contribute to this suboptimal performance. Firstly, the system's efficiency is declining due to the ground heat depletion meaning that the profit generated from local heating production is insufficient to cover the costs of electricity and installation. Secondly, the nature of low-temperature systems necessitates purchasing a substantial amount of HVAC equipment, such as heat pumps, wiring, and sensors, to enable local heating production. The heat production in this system relies on purchased electric energy, which is more expensive than the district heating energy. Nevertheless, the limitations of the study need to be considered, as the electricity and heat prices were fixed, and the equipment prices were taken from the 2018 economic analysis, therefore, at present, the situation might change. It should also be noted that the district heating systems typically have a longer lifetime than 20 years, only requiring the replacement of heat pumps, therefore likely changing their profitability drastically (Atkinson et al., 2009). More so, installing conventional district heating systems is economically unfeasible in areas with low population density, making the analysed system a viable alternative for the, e.g., villages or other areas distanced from the major population centres.(Persson et al., 2011)

The environmental performance of the analysed LTDH (Low-Temperature District Heating) system is mainly positive, considering that district heating in Denmark still heavily relies on fossil fuels like coal, natural gas, and oil. However, there is room for improvement in this area. Denmark's electricity production depends on fossil fuels and renewable energy sources with lower reliability, such as wind power. This reliance on fossil fuels

resulted in higher emissions from the electricity generation sector in 2021 (Johansen et al., 2022). Another challenge the analysed system faces is the occurrence of "electricity bottlenecks." These bottlenecks happen when there is a surge in electrical grid demand during hours when renewable electricity is unavailable. Incorporating local renewable electricity generation into the system could be beneficial to address these issues. For example, installing photovoltaic panels on nearby buildings could alleviate the electricity bottleneck problem and potentially improve the system's environmental and economic efficiency. By integrating locally generated renewable energy, the system's dependence on the grid would be reduced, decreasing overall environmental impact. This approach would make the system more sustainable and cost-effective in the long run. It is worth noting that a more detailed Life Cycle Assessment (LCA) could substantially influence the results due to the significant presence of mechanical equipment within the system and its associated embodied carbon emissions.

Several avenues for future research on this system could lead to improvements and a better understanding of its performance:

- Installation of additional sensors: Installing more sensors throughout the system can help to understand its behaviour better and obtain complete data. This would provide a more comprehensive dataset for analysis, leading to more accurate conclusions and potentially revealing areas for optimisation.

- Detailed environmental analysis: Examining the environmental aspects of the system in greater depth, including equipment and energy use, can provide a clearer picture of the system's overall environmental impact. This could help identify areas where improvements can be made to reduce its carbon footprint.

- Integration of renewable electricity generation: Investigating the integration of renewable electricity generation, such as solar panels or wind turbines, can help determine the feasibility and consequences of incorporating such solutions. This could reduce the system's reliance on grid electricity and improve its environmental and economic efficiency.

- Implementation of direct free cooling implementation and heat reinjection: Assessing the possibility of implementing direct free cooling and other methods of reinjecting heat into the ground can help to boost system efficiency. The system's economic and environmental performance could be significantly improved by utilising the cooling effect of these measures.

By exploring these research directions, the system can be further optimised and its performance better understood, paving the way for more efficient, environmentally friendly, and economically viable district heating solutions.

5 Conclusions and future work

This study evaluated technical, economic and environmental aspects of the Danish low-temperature district heating grid with a bore field thermal storage. A system model has been developed and successfully validated as part of this process. This model serves as a representation of the district heating system, allowing for a deeper understanding of its functioning and behaviour. From a techno-economic standpoint, two particular improvement areas have been identified within the system. One issue of the analysed system is the depletion of heat in the bore field system over time. This depletion leads to a decline in the system's overall efficiency and impacts its economic profitability. The other issue is the system's reliance on the grid electricity, leading to potential improvement in the economic and environmental aspects. To address these issues, two potential technical solutions have been identified.

The first solution involves the introduction of direct free cooling. By implementing this approach, it is possible to mitigate or slow down the ground depletion process. Direct-free cooling utilizes the colder temperatures available in the external environment, such as during winter months, to provide cooling to the system. This solution could also help to preserve the stored heat in the bore field system and reduce its depletion rate. Additionally, the recovered energy from the cooling process can be utilized to enhance the thermal comfort of the system's end users. By maximizing the utilization of the available resources, the system can optimize its performance and efficiency.

The second solution focuses on the integration of renewable electricity production. This integration has the potential to improve both the environmental and economic performance of the district heating system. By utilizing renewable energy sources, such as solar or wind power, to generate electricity, the system can reduce its reliance on conventional and non-renewable energy sources, decreasing its carbon footprint and increasing its profitability. Moreover, the integration of renewable electricity production can enhance the energy resilience of the region by diversifying the energy mix and reducing dependence on external energy sources. These measures could contribute to a more sustainable and efficient district heating system, benefiting the local community and the environment.

References

Abel, E. (1994). Low-energy buildings. *Energy and Buildings*, *21*(3), 169–174. https://doi.org/10.1016/0378-7788(94)90032-9

Abugabbara, M., Alberdi-Pagola, M., Javed, S., & Poulsen, S. E. (2022, October). Integration of ground-source heat pumps in combined district heating and cooling networks: A holistic modeling framework. *European Geothermal Congress 2022*. https://www.ucviden.dk/en/publications/integration-of-ground-source-heat-pumps-in-combined-district-heat

Abugabbara, M., Javed, S., & Johansson, D. (2022). A simulation model for the design and analysis of district systems with simultaneous heating and cooling demands. *Energy*, *261*, 125245. https://doi.org/10.1016/J.ENERGY.2022.125245

Andersen, S. S. (2017, August 3). *Revitalisering af landdistrikterne via termonettet*. Termonet Danmark. https://termonet.dk/artikler/revitalisering-af-landdistrikterne-via-termonettet/

ASHRAE. (2013). *District heating guide*. American Society of Heating, Refrigerating and Air-Conditioning Engineers, Inc. https://www.techstreet.com/ashrae/standards/district-heating-and-cooling-guides?ashrae_auth_token=&gateway_code=ashrae&product_id=1863051

ASHRAE. (2017). CHAPTER 19: Energy estimating and modeling methods. In *2017 Ashrae Handbook -- Fundamentals (Si)* (2017th ed., p. 19.34). https://books.google.com/books/about/2017_ASHRAE_Handbook.html?hl=ru&id=6VhRswEACAAJ

Atkinson, J. G. B., Jackson, T., & Mullings-Smith, E. (2009). Market influence on the low carbon energy refurbishment of existing multi-residential buildings. *Energy Policy*, *37*(7), 2582–2593. https://doi.org/10.1016/J.ENPOL.2009.02.025

Averfalk, H., & Werner, S. (2020). Economic benefits of fourth generation district heating. *Energy*, *193*, 116727. https://doi.org/10.1016/J.ENERGY.2019.116727

Baldvinsson, I., & Nakata, T. (2016). A feasibility and performance assessment of a low temperature district heating system – A North Japanese case study. *Energy*, *95*, 155–174. https://doi.org/10.1016/J.ENERGY.2015.11.057

Bauer, D., Heidemann, W., Müller-Steinhagen, H., & Diersch, H. J. G. (2011). Thermal resistance and capacity models for borehole heat exchangers. *International Journal of Energy Research*, *35*(4), 312–320. https://doi.org/10.1002/ER.1689

Bober, W. (2013). Introduction to Numerical and Analytical Methods with MATLAB® for Engineers and Scientists. In W. Bober (Ed.), *Introduction to Numerical and Analytical Methods with MATLAB* (1st ed.). CRC Press. https://doi.org/10.1201/B16030/INTRODUCTION-NUMERICAL-ANALYTICAL-METHODS-MATLAB-ENGINEERS-SCIENTISTS-WILLIAM-BOBER

Buffa, S., Cozzini, M., D'Antoni, M., Baratieri, M., & Fedrizzi, R. (2019). 5th generation district heating and cooling systems: A review of existing cases in Europe. *Renewable and Sustainable Energy Reviews*, *104*, 504–522. https://doi.org/10.1016/J.RSER.2018.12.059

Cimmino, M. (2018). Fast calculation of the g-functions of geothermal borehole fields using similarities in the evaluation of the finite line source solution. *Https://Doi.Org/10.1080/19401493.2017.1423390*, *11*(6), 655–668. https://doi.org/10.1080/19401493.2017.1423390

Cimmino, M., & Bernier, M. (2014). A semi-analytical method to generate g-functions for geothermal bore fields. *International Journal of Heat and Mass Transfer*, *70*, 641–650. https://doi.org/10.1016/J.IJHEATMASSTRANSFER.2013.11.037

Claesson, J., & Javed, S. (2012). A Load-Aggregation Method to Calculate Extraction Temperatures of Borehole Heat Exchangers. *Ashrae Transactions*.

Connolly, D., Lund, H., & Mathiesen, B. V. (2016). Smart Energy Europe: The technical and economic impact of one potential 100% renewable energy scenario for the European Union.

Renewable and Sustainable Energy Reviews, *60*, 1634–1653. https://doi.org/10.1016/J.RSER.2016.02.025

Dalla Rosa, A., Boulter, R., Church, K., & Svendsen, S. (2012). District heating (DH) network design and operation toward a system-wide methodology for optimizing renewable energy solutions (SMORES) in Canada: A case study. *Energy*, *45*(1), 960–974. https://doi.org/10.1016/j.energy.2012.06.062

Egebo, T., & Thyregod, T. (2022). *Energinet miljødeklaration 2021*. https://energinet.dk/media/52hd5mv0/miljdeklarationen-samlet-dokument.pdf

Eskilson, P. (1987). *Thermal analysis of heat extraction boreholes* [Lund University]. https://portal.research.lu.se/en/publications/thermal-analysis-of-heat-extraction-boreholes

Fang, H., Xia, J., & Jiang, Y. (2015). Key issues and solutions in a district heating system using low-grade industrial waste heat. *Energy*, *86*, 589–602. https://doi.org/10.1016/J.ENERGY.2015.04.052

Filonenko, K., Arendt, K., Jradi, M., Andersen, S., & Veje, C. (2019). Modeling and simulation of a heating mini-grid for a block of buildings. *Building Simulation Conference Proceedings*, *3*, 1971–1978. https://doi.org/10.26868/25222708.2019.210870

Fleiter, T., Steinbach, J., & Ragwitz, M. (2017). *Mapping and analyses of the current and future (2020 - 2030) heating/cooling fuel deployment (fossil/renewables)*.

Fragaki, A., Andersen, A. N., & Toke, D. (2008). Exploration of economical sizing of gas engine and thermal store for combined heat and power plants in the UK. *Energy*, *33*(11), 1659–1670. https://doi.org/10.1016/J.ENERGY.2008.05.011

Fulghum, N. (2023). *Yearly electricity data*. Ember Climate. https://ember-climate.org/data-catalogue/yearly-electricity-data/

Gjoka, K., Rismanchi, B., & Crawford, R. H. (2023). Fifth-generation district heating and cooling systems: A review of recent advancements and implementation barriers. *Renewable and Sustainable Energy Reviews*, *171*, 112997. https://doi.org/10.1016/J.RSER.2022.112997

Green Delta. (2015, January). *openLCA.org*. Green Delta LCA Analysis Method: CML Non-Baseline - GWP100 GWP. https://www.openlca.org/download

Gudmundsson, O., Schmidt, R. R., Dyrelund, A., & Thorsen, J. E. (2022). Economic comparison of 4GDH and 5GDH systems – Using a case study. *Energy*, *238*, 121613. https://doi.org/10.1016/J.ENERGY.2021.121613

International Energy Agency. (2018). *The Future of Cooling – Analysis - IEA*. https://www.iea.org/reports/the-future-of-cooling

International Energy Agency. (2022, September). *Heating – Analysis - IEA*. https://www.iea.org/reports/heating

International Energy Agency. (2023, April). *World Energy Balances*. https://www.iea.org/data-and-statistics/data-product/world-energy-balances#energy-balances

Javed, S., & Spitler, J. D. (2022). Vertical ground heat exchanger pressure loss – Experimental comparisons and calculation procedures. *Geothermics*, *105*, 102546. https://doi.org/10.1016/J.GEOTHERMICS.2022.102546

Johansen, K., & Werner, S. (2022). Something is sustainable in the state of Denmark: A review of the Danish district heating sector. *Renewable and Sustainable Energy Reviews*, *158*, 112117. https://doi.org/10.1016/J.RSER.2022.112117

Karlsson, J. F., & Moshfegh, B. (2007). A comprehensive investigation of a low-energy building in Sweden. *Renewable Energy*, *32*(11), 1830–1841. https://doi.org/10.1016/J.RENENE.2006.10.009

Kvisgaard, B., & Hadvig, S. (1980). *Varmetab fra fjernvarmeledninger : Heat loss from pipelines in district heating systems*.

Kwon, P. S., & Østergaard, P. (2014). Assessment and evaluation of flexible demand in a Danish future energy scenario. *Applied Energy*, *134*, 309–320. https://doi.org/10.1016/J.APENERGY.2014.08.044

Laferrière, A., Cimmino, M., Picard, D., & Helsen, L. (2020). Development and validation of a full-time-scale semi-analytical model for the short- and long-term simulation of vertical geothermal bore fields. *Geothermics*, *86*, 101788. https://doi.org/10.1016/J.GEOTHERMICS.2019.101788

Lauster, M., Teichmann, J., Fuchs, M., Streblow, R., & Mueller, D. (2014). Low order thermal network models for dynamic simulations of buildings on city district scale. *Building and Environment*, *73*, 223–231. https://doi.org/10.1016/J.BUILDENV.2013.12.016

Li, D. H. W., Yang, L., & Lam, J. C. (2012). Impact of climate change on energy use in the built environment in different climate zones – A review. *Energy*, *42*(1), 103–112. https://doi.org/10.1016/J.ENERGY.2012.03.044

Li, M., Li, P., Chan, V., & Lai, A. C. K. (2014). Full-scale temperature response function (G-function) for heat transfer by borehole ground heat exchangers (GHEs) from sub-hour to decades. *Applied Energy*, *136*, 197–205. https://doi.org/10.1016/j.apenergy.2014.09.013

Lindhe, J., Javed, S., Johansson, D., & Bagge, H. (2022). A review of the current status and development of 5GDHC and characterization of a novel shared energy system. *Https://Doi.Org/10.1080/23744731.2022.2057111*, *28*(5), 595–609. https://doi.org/10.1080/23744731.2022.2057111

Liu, H., Zhang, H., & Javed, S. (2020). Long-Term Performance Measurement and Analysis of a Small-Scale Ground Source Heat Pump System. *Energies 2020, Vol. 13, Page 4527*, *13*(17), 4527. https://doi.org/10.3390/EN13174527

Long, N., Gautier, A., Elarga, H., Allen, A., Summer, T., Klun, L., Moore, N., & Wetter, M. (2021). Modeling district heating and cooling systems with URBANopt, GeoJSON to Modelica Translator, and the Modelica Buildings Library. *Proceedings of Building Simulation 2021: 17th Conference of IBPSA*, *17*, 2187–2194. https://doi.org/10.26868/25222708.2021.30943

Lottner, V., Schulz, M. E., & Hahne, E. (2000). Solar-Assisted District Heating Plants: Status of the German Programme Solarthermie-2000. *Solar Energy*, *69*(6), 449–459. https://doi.org/10.1016/S0038-092X(00)00125-0

Lund, H., Andersen, A. N., Østergaard, P. A., Mathiesen, B. V., & Connolly, D. (2012). From electricity smart grids to smart energy systems - A market operation based approach and understanding. *Energy*, *42*(1), 96–102. https://doi.org/10.1016/J.ENERGY.2012.04.003

Lund, H., Hvelplund, F., Mathiesen, B., & Østergaard, P. (2011). Coherent energy and environmental system analysis. *Downloaded from Orbit.Dtu.Dk On*, *25*, 2023. https://orbit.dtu.dk/files/9739523/Coherent_energy.pdf

Lund, H., Möller, B., Mathiesen, B. V., & Dyrelund, A. (2010). The role of district heating in future renewable energy systems. *Energy*, *35*(3), 1381–1390. https://doi.org/10.1016/J.ENERGY.2009.11.023

Lund, H., Østergaard, P. A., Nielsen, T. B., Werner, S., Thorsen, J. E., Gudmundsson, O., Arabkoohsar, A., & Mathiesen, B. V. (2021). Perspectives on fourth and fifth generation district heating. *Energy*, *227*, 120520. https://doi.org/10.1016/J.ENERGY.2021.120520

Lund, H., Šiupšinskas, G., & Martinaitis, V. (2005). Implementation strategy for small CHP-plants in a competitive market: the case of Lithuania. *Applied Energy*, *82*(3), 214–227. https://doi.org/10.1016/J.APENERGY.2004.10.013

Lund, H., Werner, S., Wiltshire, R., Svendsen, S., Thorsen, J. E., Hvelplund, F., & Mathiesen, B. V. (2014). 4th Generation District Heating (4GDH): Integrating smart thermal grids into future sustainable energy systems. *Energy*, *68*, 1–11. https://doi.org/10.1016/J.ENERGY.2014.02.089

Marsh, R., Larsen, V. G., & Kragh, M. (2009). Housing and energy in Denmark: past, present, and future challenges. *Https://Doi.Org/10.1080/09613210903226608*, *38*(1), 92–106. https://doi.org/10.1080/09613210903226608

Mathys, W., Stanke, J., Harmuth, M., & Junge-Mathys, E. (2008). Occurrence of Legionella in hot water systems of single-family residences in suburbs of two German cities with special reference to solar and district heating. *International Journal of Hygiene and Environmental Health*, *211*(1–2), 179–185. https://doi.org/10.1016/J.IJHEH.2007.02.004

Modelica Association. (2023). *Modelica* (3.6). Modelica Association. https://modelica.org/

Musić, J., & Zupančič, B. (2006). Modeling , Simulation and Control of Inverted Pendulum on a Chart Using Object Oriented Approach with Modelica. *Electrotechnical and and Computer Science Conference ERK 2006*.

Nastasi, B., & Lo Basso, G. (2016). Hydrogen to link heat and electricity in the transition towards future Smart Energy Systems. *Energy*, *110*, 5–22. https://doi.org/10.1016/J.ENERGY.2016.03.097

Ommen, T., Markussen, W. B., & Elmegaard, B. (2016). Lowering district heating temperatures – Impact to system performance in current and future Danish energy scenarios. *Energy*, *94*, 273–291. https://doi.org/10.1016/J.ENERGY.2015.10.063

Ozgener, L., Hepbasli, A., & Dincer, I. (2005). Energy and exergy analysis of geothermal district heating systems: an application. *Building and Environment*, *40*(10), 1309–1322. https://doi.org/10.1016/J.BUILDENV.2004.11.001

Perry, S., Klemeš, J., & Bulatov, I. (2008). Integrating waste and renewable energy to reduce the carbon footprint of locally integrated energy sectors. *Energy*, *33*(10), 1489–1497. https://doi.org/10.1016/J.ENERGY.2008.03.008

Persson, U., & Werner, S. (2011). Heat distribution and the future competitiveness of district heating. *Applied Energy*, *88*(3), 568–576. https://doi.org/10.1016/J.APENERGY.2010.09.020

Picard, D., & Helsen, L. (2014). Advanced Hybrid Model for Borefield Heat Exchanger Performance Evaluation, an Implementation in Modelica. *Proceedings of the 10th International Modelica Conference, March 10-12, 2014, Lund, Sweden*, *96*, 857–866. https://doi.org/10.3384/ECP14096857

Psomas, T., Heiselberg, P., Duer, K., & Bjørn, E. (2016). Overheating risk barriers to energy renovations of single family houses: Multicriteria analysis and assessment. *Energy and Buildings*, *117*, 138–148. https://doi.org/10.1016/J.ENBUILD.2016.02.031

Qiao, Y., & Kajbaf Nezhad, M. (2021). Pipe Surface Roughness at Microscale and Discussion of Possible Relation to Flow Properties [Lund University]. In *TVVR21/5014; (2021)*. http://lup.lub.lu.se/student-papers/record/9056647

Ropenus, S., & Klinge Jacobsen, H. (2015). A Snapshot of the Danish Energy Transition: Objectives, Markets, Grid, Support Schemes and Acceptance. Study. *Uniwersytet Śląski*, *7*(1), 343–354. https://doi.org/10.2/JQUERY.MIN.JS

Sangi, R., Jahangiri, P., Thamm, A., & Müller, D. (2017). Dynamic exergy analysis – Modelica®-based tool development: A case study of CHP district heating in Bottrop, Germany. *Thermal Science and Engineering Progress*, *4*, 231–240. https://doi.org/10.1016/J.TSEP.2017.10.008

Sayegh, M. A., Danielewicz, J., Nannou, T., Miniewicz, M., Jadwiszczak, P., Piekarska, K., & Jouhara, H. (2017). Trends of European research and development in district heating technologies. *Renewable and Sustainable Energy Reviews*, *68*, 1183–1192. https://doi.org/10.1016/J.RSER.2016.02.023

Schmidt, D., Kallert, A., Blesl, M., Svendsen, S., Li, H., Nord, N., & Sipilä, K. (2017). Low Temperature District Heating for Future Energy Systems. *Energy Procedia*, *116*, 26–38. https://doi.org/10.1016/J.EGYPRO.2017.05.052

Schweiger, G., Larsson, P. O., Magnusson, F., Lauenburg, P., & Velut, S. (2017). District heating and cooling systems – Framework for Modelica-based simulation and dynamic optimization. *Energy*, *137*, 566–578. https://doi.org/10.1016/J.ENERGY.2017.05.115

Smil, V., & BP Statistical Review of World Energy. (2022, June). *Global direct primary energy consumption*. https://ourworldindata.org/grapher/global-primary-energy?country=~OWID_WRL

Sommer, T., Sulzer, M., Wetter, M., Sotnikov, A., Mennel, S., & Stettler, C. (2020). The reservoir network: A new network topology for district heating and cooling. *Energy*, *199*, 117418. https://doi.org/10.1016/J.ENERGY.2020.117418

Soons, F. F. M., Galdiz, J. I. T., Hensen, J. L. M., & Schrevel, R. A. M. de. (2014). A Modelica based computational model for evaluating a renewable district heating system. *Title of Host PublicationProceedings of the 9th International Conference on System Simulation in Buildings*,

1–16. https://research.tue.nl/en/publications/a-modelica-based-computational-model-for-evaluating-a-renewable-d

Swedish Institute for Standards. (2019). SS-EN 13941-2:2019+A1:2021. In *District heating pipes - Design and installation of thermal insulated bonded single and twin pipe systems for directly buried hot water networks - Part 2: Installation* (Vol. 2). Swedish Institute for Standards. https://www.sis.se/en/produkter/energy-and-heat-transfer-engineering/heat-recovery-thermal-insulation/ss-en-13941-22019a12021/

Thomsen, K. E., Schultz, J. M., & Poel, B. (2005). Measured performance of 12 demonstration projects—IEA Task 13 "advanced solar low energy buildings". *Energy and Buildings*, *37*(2), 111–119. https://doi.org/10.1016/J.ENBUILD.2004.01.036

Thorsen, J. E., Gudmudsson, O., Brand, M., & Dyrelund, A. (2020). Distribution of district heating: 3rd Generation. In *Danfoss - District heating generations explained*.

Thorsen, J. E., Gudmundsson, O., Brand, M., & Dyrelund, A. (2020). *Distribution of district heating: 2nd Generation*. www.danfoss.com

Tiwari, S. (2011). *Professional NoSQ* (R. Elliot, S. Jones, S. Edlich, M. Ingenthron, D. Scribner, & K. Coffer, Eds.; 1st ed., Vol. 1st). John Wiley & Sons Inc. https://www.amazon.com/Professional-NoSQL-Shashank-Tiwari/dp/047094224X

Torchio, M. F., Genon, G., Poggio, A., & Poggio, M. (2009). Merging of energy and environmental analyses for district heating systems. *Energy*, *34*(3), 220–227. https://doi.org/10.1016/J.ENERGY.2008.01.012

Dataindsamling fra danske termonet (HO5), (2022). https://www.coolgeoheat.eu/siteassets/publikationer/h05/13.-driftsdata_fra_termonet_balle-bygade-silkeborg.pdf

van der Heijde, B., Aertgeerts, A., & Helsen, L. (2017). Modelling steady-state thermal behaviour of double thermal network pipes. *International Journal of Thermal Sciences*, *117*, 316–327. https://doi.org/10.1016/J.IJTHERMALSCI.2017.03.026

Volkova, A., Latõšov, E., Lepiksaar, K., & Siirde, A. (2020). Planning of district heating regions in Estonia. *International Journal of Sustainable Energy Planning and Management*, *27*(Special Issue), 5–15. https://doi.org/10.5278/IJSEPM.3490

Volkova, A., Pakere, I., Murauskaite, L., Huang, P., Lepiksaar, K., & Zhang, X. (2022). 5th generation district heating and cooling (5GDHC) implementation potential in urban areas with existing district heating systems. *Energy Reports*, *8*, 10037–10047. https://doi.org/10.1016/J.EGYR.2022.07.162

von Rhein, J., Henze, G. P., Long, N., & Fu, Y. (2019). Development of a topology analysis tool for fifth-generation district heating and cooling networks. *Energy Conversion and Management*, *196*, 705–716. https://doi.org/10.1016/J.ENCONMAN.2019.05.066

Wallentén, P. (1991). *Steady-state heat loss from insulated pipes*. Lund University.

Wang, G., & Tang, J. (2012). The NoSQL principles and basic application of cassandra model. *Proceedings - 2012 International Conference on Computer Science and Service System, CSSS 2012*, 1332–1335. https://doi.org/10.1109/CSSS.2012.336

Wang, P. G., Scharling, M., Nielsen, K. P., Kern-Hansen, C., & Wittchen, K. B. (2013). 2001 – 2010 Danish Design Reference Year: Reference Climate Dataset for Technical Dimensioning in Building, Construction and other Sectors. In *Danmarks Meteorologiske Institut. DMI Technical Report*. Danmarks Meteorologiske Institut. https://vbn.aau.dk/en/publications/2001-2010-danish-design-reference-year-reference-climate-dataset-

Werner, S. (2017). District heating and cooling in Sweden. *Energy*, *126*, 419–429. https://doi.org/10.1016/J.ENERGY.2017.03.052

Wetter, M., Zuo, W., Nouidui, T. S., & Pang, X. (2014). Modelica Buildings library. *Journal of Building Performance Simulation*, *7*(4), 253–270. https://doi.org/10.1080/19401493.2013.765506

Wirtz, M., Kivilip, L., Remmen, P., & Müller, D. (2020). 5th Generation District Heating: A novel design approach based on mathematical optimization. *Applied Energy*, *260*, 114158. https://doi.org/10.1016/J.APENERGY.2019.114158

Wirtz, M., Neumaier, L., Remmen, P., & Müller, D. (2021). Temperature control in 5th generation district heating and cooling networks: An MILP-based operation optimization. *Applied Energy*, *288*, 116608. https://doi.org/10.1016/J.APENERGY.2021.116608

Wirtz, M., Schreiber, T., & Müller, D. (2022). Survey of 53 Fifth-Generation District Heating and Cooling (5GDHC) Networks in Germany. *Energy Technology*, *10*(11), 2200749. https://doi.org/10.1002/ENTE.202200749

Yang, X., Li, H., & Svendsen, S. (2016). Decentralized substations for low-temperature district heating with no Legionella risk, and low return temperatures. *Energy*, *110*, 65–74. https://doi.org/10.1016/J.ENERGY.2015.12.073

Zhu, L., Hurt, R., Correia, D., & Boehm, R. (2009). Detailed energy saving performance analyses on thermal mass walls demonstrated in a zero energy house. *Energy and Buildings*, *41*(3), 303–310. https://doi.org/10.1016/J.ENBUILD.2008.10.003

Appendix

Table A: Cost/Revenue parameters

Parameter	Value [Unit]	Unit
Area of the building	130	[m^2]
Number of buildings	15	[-]
Number of boreholes	6	[-]
Interest rate	2.6	[%]
Discount rate	3	[%]
Analysis period	20	[years]
Heating energy price	350	[DKK/MWh]
Heat meter renting price	840	[DKK/Building]
Facility cost contribution	2 400	[DKK/Building]
Fixed fee for heating	15.2	[DKK/m^2 of the building]
Borehole drilling cost	79 746	[DKK/Borehole]
Cost of the heat pump, excluding VAT	58 867	[DKK/Heat pump]
Cost of ground works	136 693	[DKK]
Wiring cost	147 188	[DKK]
Cost of electrical units and cabling of heat pumps	8 220	[DKK/Building]
Cost of one heat meter	3 120	[DKK/Heat meter]
Cost of connection pipes excavation	6 600	[DKK/Building]
Investment contribution of one house	-7 380	[DKK/Building]
Increased investment contribution, due to heat pump installation	-29 000	[DKK/Building]
Connection pipes contribution	-18 800	[DKK/Building]
Development allowance	-275 360	[DKK]
Electricity prices, Energynet	81	[DKK/MWh]
Electricity prices, Eniig	417	[DKK/MWh]
Electricity prices, N1	191	[DKK/MWh]
Energy tax excluding VAT	155 - 255	[DKK/MWh]
Public service obligation	0 - 62	[DKK/MWh]
Water treatment cost	5	[DKK/MWh]
Wiring cost	6	[DKK/MWh]
Maintenance cost	1 750	[DKK/Building/Year]
Servicing cost	250	[DKK/Building/Year]
Administrative cost	400	

LUND UNIVERSITY

Divisions of Energy and Building Design, Building Physics and Building Services
Department of Building and Environmental Technology